SCIENCE CHINA
Physics, Mechanics & Astronomy

•Invited Review•

September 2018 Vol. 61 No. 9: 094601
https://doi.org/10.1007/s11433-018-9239-9

An overview of healthcare monitoring by flexible electronics

JianQiao Hu[1], Rui Li[2*], Yuan Liu[3], and YeWang Su[1,4,2,5*]

[1] *State Key Laboratory of Nonlinear Mechanics, Institute of Mechanics, Chinese Academy of Sciences, Beijing 100190, China;*
[2] *State Key Laboratory of Structural Analysis for Industrial Equipment, Department of Engineering Mechanics, and International Research Center for Computational Mechanics, Dalian University of Technology, Dalian 116024, China;*
[3] *Applied Mechanics Laboratory, School of Aerospace Engineering, Tsinghua University, Beijing 100084, China;*
[4] *School of Engineering Science, University of Chinese Academy of Sciences, Beijing 100049, China;*
[5] *State Key Laboratory of Digital Manufacturing Equipment and Technology, Huazhong University of Science and Technology, Wuhan 430074, China*

Received April 2, 2018; accepted May 4, 2018; published online July 10, 2018

Flexible electronics integrated with stretchable/bendable structures and various microsensors that monitor the temperature, pressure, sweat, bioelectricity, body hydration, etc., have a wide range of applications in the human healthcare sector. The science underlying this technology draws from many research areas, such as information technology, materials science, and structural mechanics, to efficiently and accurately monitor technology for various signals. In this paper, we make a classification and comb to the designs, materials, structures and functions of numerous flexible electronics for signal monitoring in the human healthcare sector. Some perspectives in this field are discussed in the concluding remarks.

flexible electronics, stretchable electronics, signal monitoring, human healthcare

PACS number(s): 42.82.Cr, 07.07.Df, 87.80.Tq, 07.50.-e

Citation: J. Q. Hu, R. Li, Y. Liu, and Y. W. Su, An overview of healthcare monitoring by flexible electronics, Sci. China-Phys. Mech. Astron. **61**, 094601 (2018), https://doi.org/10.1007/s11433-018-9239-9

1 Introduction

Over the past two decades, intelligentization and informatization have become increasingly popular in the development of science and technology. A large number of microsensors and actuators have been integrated into all aspects of electronic devices. Microelectronics has become a core sector in the development of information technology. By achieving flexibility and stretchability, microelectronics can greatly expand the current application scenarios. Therefore, flexible electronics, which integrates electronics, materials science, mechanics, physics, and other such fields, have immense potential in various applications, such as electronic eye cameras [1,2], electronic skins [3,4], flexible health monitors [5], and scalable ion batteries [6]. The main advantage of flexible electronics is its ability to fit into a variety of complex surfaces, such as the human skin, which makes it possible to manufacture wearable devices for human healthcare. According to Transparency Market Research, the global biosensors market was valued at $9.9 billion in 2011, and it is expected to reach as high as $18.9 billion by 2018 [7]. With potential thousands of new wearable devices being developed over the coming decade, both academia and industry have invested a lot of resources in this field. Research on flexible electronic devices in the field of

*Corresponding authors (Rui Li, email: ruili@dlut.edu.cn, YeWang Su, email: yewangsu@imech.ac.cn)

healthcare includes two main aspects: (1) stretchability for withstanding large deformations through mechanical analyses and designs and (2) accurate monitoring and feedback of various physiological signals.

Two basic ideas underlie the design and fabrication of stretchable electronic devices. The first exploits new materials that can withstand large deformations. This concept promotes the investigation of organic electronics [8]. However, organic materials have lower electrical performance and shorter service life [9]. To overcome these challenges, another strategy to enhance the flexibility and stretchability of inorganic electronics has been proposed by a series of elaborate mechanical designs [10-13]. This approach combines high-quality electronic materials, such as inorganic semiconductor materials with the flexible substrates, to achieve flexibility and stretchability for the entire device. Despite considerable success in mechanical design, further research is needed on the functional components of the electronic devices for monitoring various signals, which will help extend the application of flexible electronics in human healthcare. The monitored signals are closely associated with body conditions, such as the wrist pulse, heart rate, blood glucose, and sweat/blood bioinformation. Stable and accurate physiological signals are crucial in endowing healthcare monitoring systems with real-time tracking capability. The monitoring and analyzing of these physiological signals provide a convenient and non-invasive way for disease diagnoses and health assessments.

The human body is a complex system where any pathology can exhibit appropriate physiological signals. Physiological measurements and stimulation techniques require electronic devices that can conform to the curvilinear surfaces of biological tissues and accommodate their large deformations. The skin is the largest organ in the human body. Changes in the properties of human skin are of great interest in the dermatology and cosmetic industries [14]. There are numerous basic physiological indicators that can reflect the physiological conditions of the human body. Figure 1 shows the various physiological signals, including temperature, pressure, sweat, bioelectricity, and hydration. The measurements of various physiological signals, especially when coupled with further analysis of the biomarkers, provide a wide range of opportunities for future practical applications.

In this paper, we review the recent advances in flexible and stretchable electronics that are currently used for electronic skins and biological devices in human healthcare. We have provided a detailed description of how various signals of the human body are monitored. The materials, structures, and functionalities of a variety of biological sensors are introduced. It is expected that this discussion will provide potential ideas for commercial applications. Some perspectives on future research opportunities have also been included.

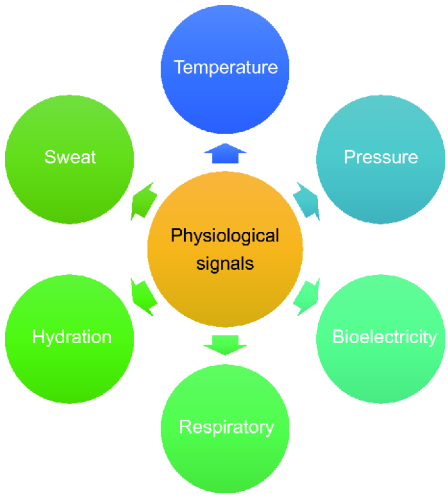

Figure 1 (Color online) Categories of commonly detectable physiological signals.

2 Signal monitoring by flexible electronics

Flexible electronics provides circuits with the capacity to withstand the strain of high level (>>1%) deformations without fracture or significant degradation of their electronic properties. Over the past several years, many impressive potential applications of these electronic devices have emerged, particularly in the area of biomedical and wearable devices [15-17]. Furthermore, a large number of related patents have been authorized. Signal monitoring is crucial for different application scenarios of flexible electronic devices. In this section, some examples of device-level demonstrations are provided by categorizing signals based on human physiological indicators.

2.1 Temperature monitoring

Human body temperature is a basal index in physiology because of its importance and close relationship with various human body lesions. Long-term real-time monitoring of temperature is of great significance in clinical medicine, especially for tracking the healthcare quality of new-born babies or patients under anesthesia. Over the past decades, several types of temperature sensors have been reported [18-20]. Figure 2(a) shows the different methods for measuring temperature, including the contact and non-contact measurement techniques. Traditionally, body temperature was taken to be the axillary temperature measured by a mercury thermometer. However, this method is not suitable or convenient for the babies or patients who are not able to keep still. A method currently used to quickly and non-invasively measure the body temperature is based on non-contacting infrared thermometers [21]; however, such devices involve high costs and cannot accurately monitor the local temperature. A feasible and practical solution is flexible and

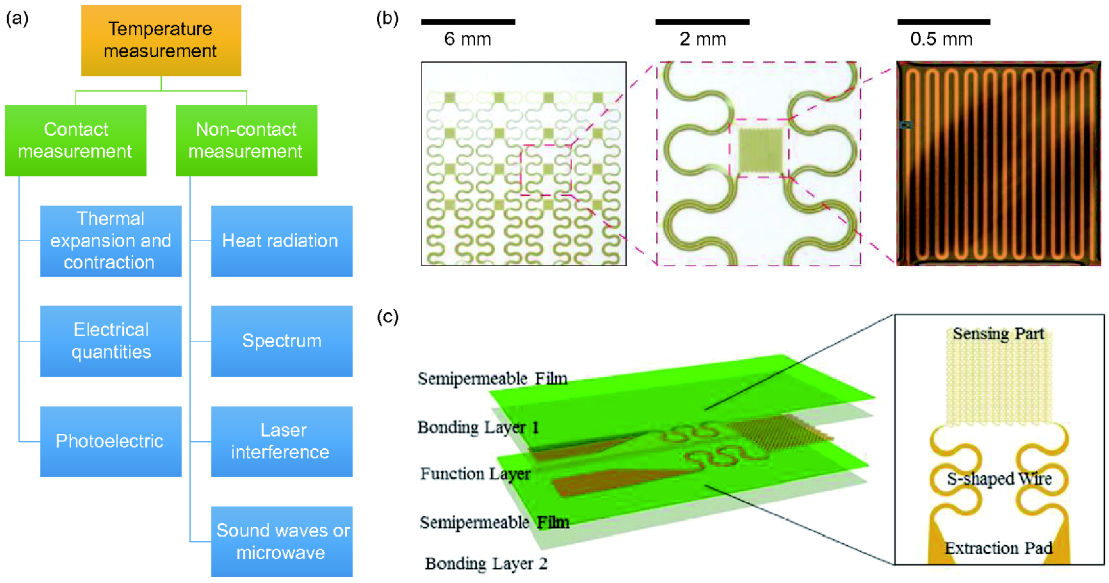

Figure 2 (Color online) (a) Different methods of temperature measurement; (b) optical images of a sensor array integrated on a thin elastomeric substrate [24]; (c) structure of an ultra-flexible temperature sensor on a breathable film [25].

wearable temperature equipment. The epidermal temperature sensors can be conformably adhered to the skin and can accurately measure the body temperature by minimizing the environmental influences. Based on the aforementioned concept of epidermal electronics, various wearable temperature sensors have been developed [22,23]; these sensors are expected to play an important role in disease diagnosis and human healthcare.

The operating principle to prepare a temperature sensor is to develop different thermo-sensitive materials. In most cases, the temperature is deduced by measuring the resistance changes of the sensor, which arise from temperature variations. Sensors based on this principle have stable performance and high reliability. An ultrathin and compliant skin-like temperature sensor was introduced based on PIN diodes made of silicon nanomembranes [24], as shown in Figure 2(b). This epidermal sensor could provide continuous and accurate thermal characterizations, including temperature contours. Chen et al. [25] fabricated a biocompatible temperature sensor by integrating temperature-sensitive materials with a semipermeable polyurethane film; this sensor had excellent accuracy as compared with a mercury thermometer. The elaborate structural design and material selection enabled the device to be breathable for the user when laminated onto the surface of the human skin (see Figure 2(c)). The biocompatibility and safety of the device have been further demonstrated by 24 h of wearing. Subsequently, Zhang et al. [26] proposed a noninvasive and continuous measurement of the core body temperature based on the temperature sensor array; they established a theoretical approach for multiple differential measurements from the sensor array. Fundamental investigations on the sensitivity, response time, and accuracy were also conducted via the analytical, numerical, and experimental approaches. More recently, a highly accurate temperature sensor based on polysilicon thermistors has been developed for monitoring brain temperature with high spatial resolution [27], and this temperature sensor has a response time of 1.5 s and sensitivity of $-0.0031°C^{-1}$.

Besides the most popular resistive temperature sensors, some other mechanisms have also attracted considerable attention because of their rapid response speeds and high resolutions. For example, a pyroelectric sensor element was developed based on a composite foil of piezoelectric ceramic lead titanate nanoparticles [28]; this element helped achieve bifunctionality of temperature and pressure changes. Mahadeva et al. [29] developed a flexible capacitive-type temperature sensor by making cellulose-polypyrrole nanocomposite; they found that the capacitance of the device increased linearly with increasing temperature. These temperature sensors can be integrated into the flexible electronic devices that monitor the continuous thermal characterization of the human body. To improve the thermal sensibility of conventional sensors, a graphene nanowall-based temperature sensor was fabricated by the plasma-enhanced chemical vapor deposition technique and the polymer-assisted transfer method [30]. The temperature coefficient of resistivity of this device was as high as $0.214°C^{-1}$, which was three times higher than that of its conventional counterparts; this showed that the device had fast response and recovery speed and excellent long-term stability.

In addition, device-level flexible temperature electronics have been widely proposed and fabricated. As illustrated in Figure 3(a), a temperature-sensor array was fabricated by

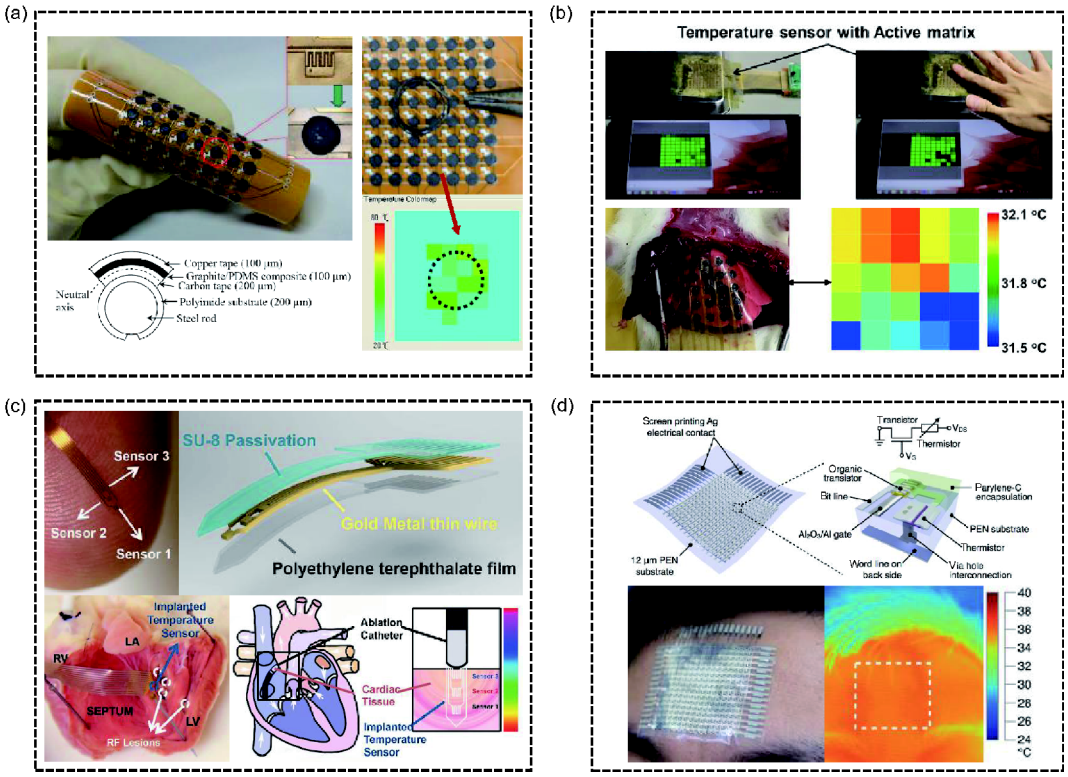

Figure 3 (Color online) (a) A temperature-sensor array and temperature distribution subjected to a heat source [31]; (b) temperature mapping of a fingertip and a rat lung [32]; (c) ultrathin injectable thermal sensors and a device injected into the myocardial tissue [33]; (d) schematic diagram of a flexible temperature sensor and the measured temperature distribution of the forehead [34].

dispensing a graphite-polydimethylsiloxane composite on flexible polyimide films [31]. This device exhibited high temperature sensitivity in a wide dynamic range from 30°C to 110°C, and the temperature distributions under different heat sources have also been measured. Subsequently, a printable thermal sensor based on the composites of semi-crystalline acrylate polymers and graphite was reported [32]. Using this device, the real-time measurement of temperature distribution at the fingertip contact as well as the temperature mapping of a rat lung was performed (see Figure 3(b)). Koh et al. [33] introduced an injectable device platform that supported precision sensors of temperature and thermal transport properties, as shown in Figure 3(c). This flexible system can be inserted into the myocardial tissue in a minimally invasive manner, which provides improved insights into lesion transmurality. Ren et al. [34] demonstrated another temperature sensor array based on large-area flexible organic field-effect transistors, as shown in Figure 3(d); these arrays allowed temperature to change from 20°C to 100°C. The temperature distributions of different objects were further measured to test the effectiveness of the integrated temperature-sensor array. Efforts are still being made to develop various flexible temperature sensors and devices because these devices have a wide range of applications in sectors, such as human health management, food processing, and pharmaceutical industry.

2.2 Pressure monitoring

Flexible pressure sensors are becoming increasingly popular because of their wide potential applications in areas such as electronic skin systems [35] and diagnostics [36,37]. In general, the pressure-sensing technology can be categorized into three types: capacitive [38,39], piezoresistive [40-43], and piezoelectric [44,45]. A disadvantage of these sensors is that they generally suffer from high deformation [46] when used for monitoring human health, especially when these are directly laminated onto the skin surface. To mimic the tactile sensing properties of natural skin, large arrays of pixel pressure sensors on a flexible and stretchable substrate are required [47]. Both the structural design and material selection have been investigated over the past years to improve the sensitivity of the mechanical sensors so that they better emulate human activities and capture human motions more precisely [48,49]. In the past, studies were mostly directed toward developing pressure sensors based on either conventional silicon or biocompatible materials [50,51]. Pressure sensitivity has received substantial attention because it determines the measurement accuracy and effectiveness of the pressure sensors. Typically, capacitive pressure sensors with excellent sensitivity and short response time have been fabricated [52]; Figure 4(a) shows the device and its structural details. Dielectric elastomer polydimethylsiloxane (PDMS) is the key material for fabricating pressure-sensitive

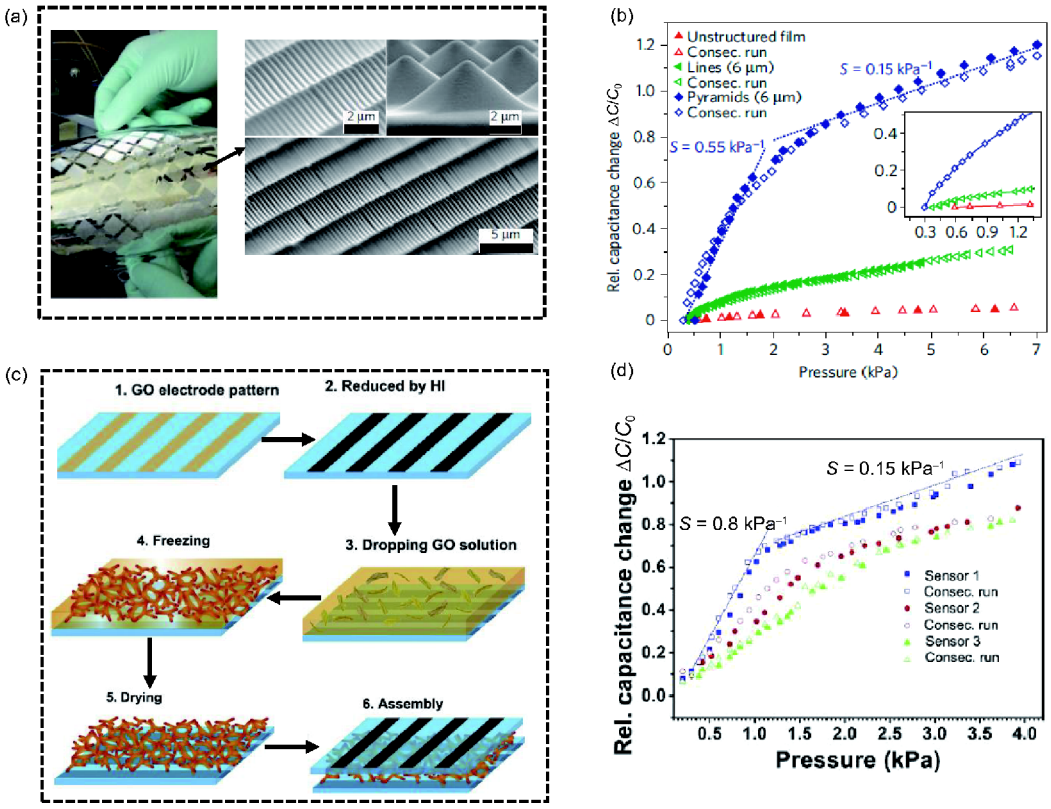

Figure 4 (Color online) (a) Pressure-sensitive structured PDMS films and the microstructured details; (b) pressure-response curves for different types of microstructured PDMS films [52]; (c) schematic of the fabrication of GO foam-based pressure sensor arrays; (d) pressure response of GO foams with different densities [53].

thin films, which are integrated with the artificial skin. However, PDMS thin films with a thickness of a few micrometers undergo significant visco-elastic creep. To overcome this, various voids have been introduced in the films to enable the microstructure surfaces to deform elastically under external pressure. The pressure response curves have been tested, and the sensitivity has improved substantially, as shown in Figure 4(b). More recently, a graphene oxide (GO)-based capacitive pressure sensor has been proposed [53]; this sensor exhibited good flexibility and robustness. The fabrication procedure for this pressure sensor is presented in Figure 4(c). The GO foam was fabricated into the sensor by sandwiching the foam between polyethyleneterephthalate (PET) sheets with patterned and reduced GO electrodes. Figure 4(d) shows how the pressure-sensing properties of the GO foam-based sensors with different GO densities were investigated.

Besides the highly sensitive capacitive-type microstructured pressure sensors, the resistive-type sensors also show tremendous promise for real applications because of their simple device structure and easy fabrication process. The performance of the resistive sensors could be based on the changes in either the resistivity of the piezoresistive materials or the contact resistance of the strain gauges upon modulation of external pressures [54-56]. Particularly, a flexible tactile sensor based on the microstructured graphene arrays was devised by combining the advantages of both graphene materials and the ordered microstructures [57], as shown in Figure 5(a). The fatigue performance or the stability of the sensor has also been deeply investigated by repeatedly applying and releasing a pressure of 100 Pa for 5000 cycles; this is shown in Figure 5(b). Subsequently, a resistive pressure sensor based on the laser-scribed graphene (LSG) has been developed [58], as shown in Figure 5(c); this sensor had high sensitivity (0.96 kPa^{-1}) in a wide pressure range (0-50 kPa). An analytical model has also been established to interpret the relationship between pressure and conductivity. This further clarified the understanding of the pressure sensor. In addition, piezoelectric pressure sensors have also been fabricated by using a GaN-based field-effect transistor [59], as shown in Figure 5(d). The pressure sensors revealed a linear response current under pressures ranging from 19.6 mN/mm^2 to 490 mN/mm^2.

After years of extensive development, flexible pressure sensor arrays are being widely applied in human healthcare and medical diagnostics, such as blood pressure, intraocular pressure, and pulse, which are significant health indicators. These sensor arrays have high resolution and rapid response beyond human perception. In particular, a stretchable pressure sensor was fabricated by employing PDMS arrays with

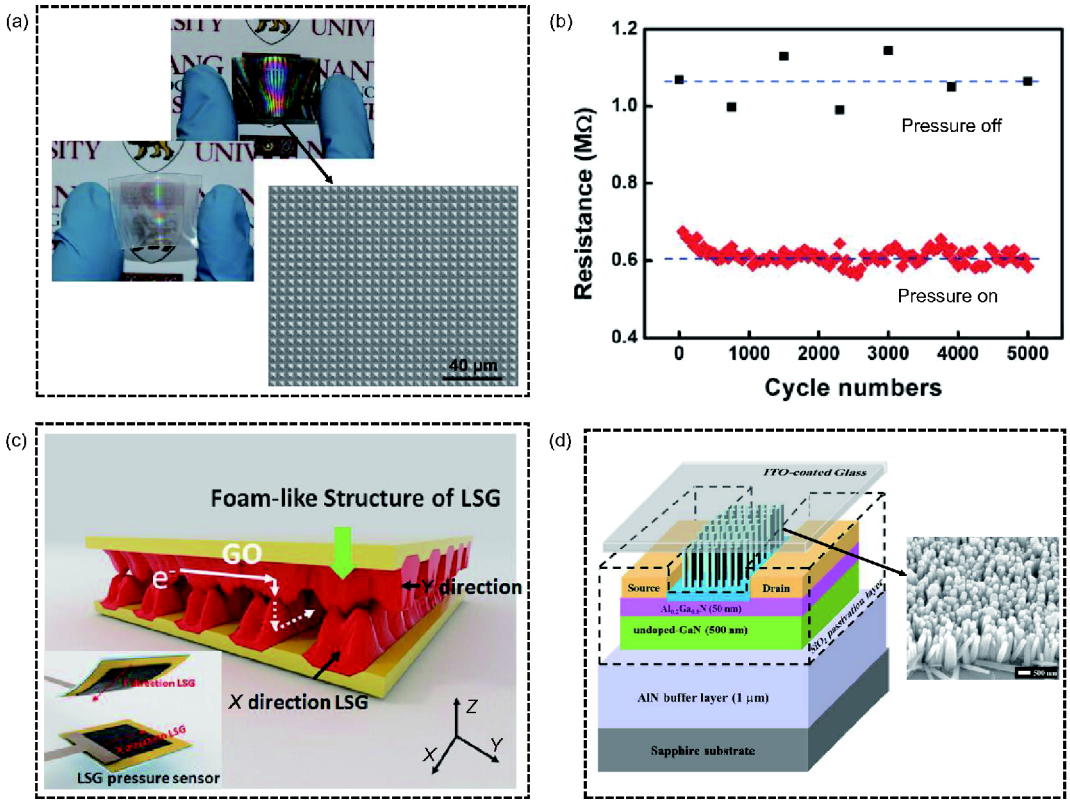

Figure 5 (Color online) (a) Photos of the PDMS films with (top right) and without (bottom left) graphene layers and the pattern arrays; (b) stability of the sensor under loading cycles [57]; (c) cross-bar device structure of the pressure sensor based on the foam-like LSG [58]; (d) epitaxial structure, schematic configuration of the pressure sensors and the SEM image of ZnO nanorod array [59].

spring-like compressible platforms [60]; the potential uses of the sensor have been further demonstrated by measuring blood pressure, as shown in Figure 6(a). A single-use biodegradable pressure sensor patch for cardiovascular monitoring and fabrication of the sensor has been reported [61] (see Figure 6(b)). The pressure sensor was attached to the carotid artery of a human subject, the arterial pulse wave and the electrocardiograph (ECG) were recorded. As shown in Figure 6(c), a smart prosthetic skin instrumented with multiplexed sensors and actuators has been demonstrated [62]; this device showed highly localized mechanical and thermal skin-like perceptions in response to various external stimuli. Furthermore, the pulse-wave measurement [63], voice vibration [64], and human activity [65] have also been monitored by the devices with collective pressure sensors (see Figure 6(d)-(f)). Figure 6(g) shows a portable sensor with a wireless transmitter capable of measuring weak signals stemming from the internal jugular vein lying deep inside the neck muscles [66]. The test results suggested that the device was able to detect the waveforms retrieved from a healthy subject and could quickly diagnose cardiovascular and cardiac illnesses.

2.3 Bioelectrical monitoring

Bioelectrical signals are now widely used for monitoring medical diagnoses and human activities. The conventional bioelectrical signals associated with the human body include electrocardiograph (ECG), electroencephalogram (EEG), electromyography (EMG), and electrooculogram (EOG). ECG signal analysis is the most widely used strategy for the continuous and non-invasive diagnosis of different cardiac diseases and for assessing the physiological fitness of athletes [67-69]. The conventional ECG signal acquisition systems generally consist of multiple biopotential electrodes that have extremely large contact impedances between the electrodes and the body skin. In the past few years, special attention has been paid to electrode improvements for obtaining better ECG signals [70-73]. Particularly, new materials and new structural designs are being developed rapidly [74]. As shown in Figure 7(a), the conductive foam that was coated with Ni/Cu reduced the surface resistance of electrodes [75]. When micro-domes were introduced on a flexible dry electrode, the impedance measurements showed that this electrode had lower skin-electrode contact impedance [76], as illustrated in Figure 7(b). Composite electrodes have also been fabricated for long-term ECG measurements [77]; these electrodes consist of a polydimethylsiloxane base, a silver nanowire layer (AgNW), and an adhesive layer, as shown in Figure 7(c). Functionalized textiles and graphene have also been used to develop graphene-clad, conductive

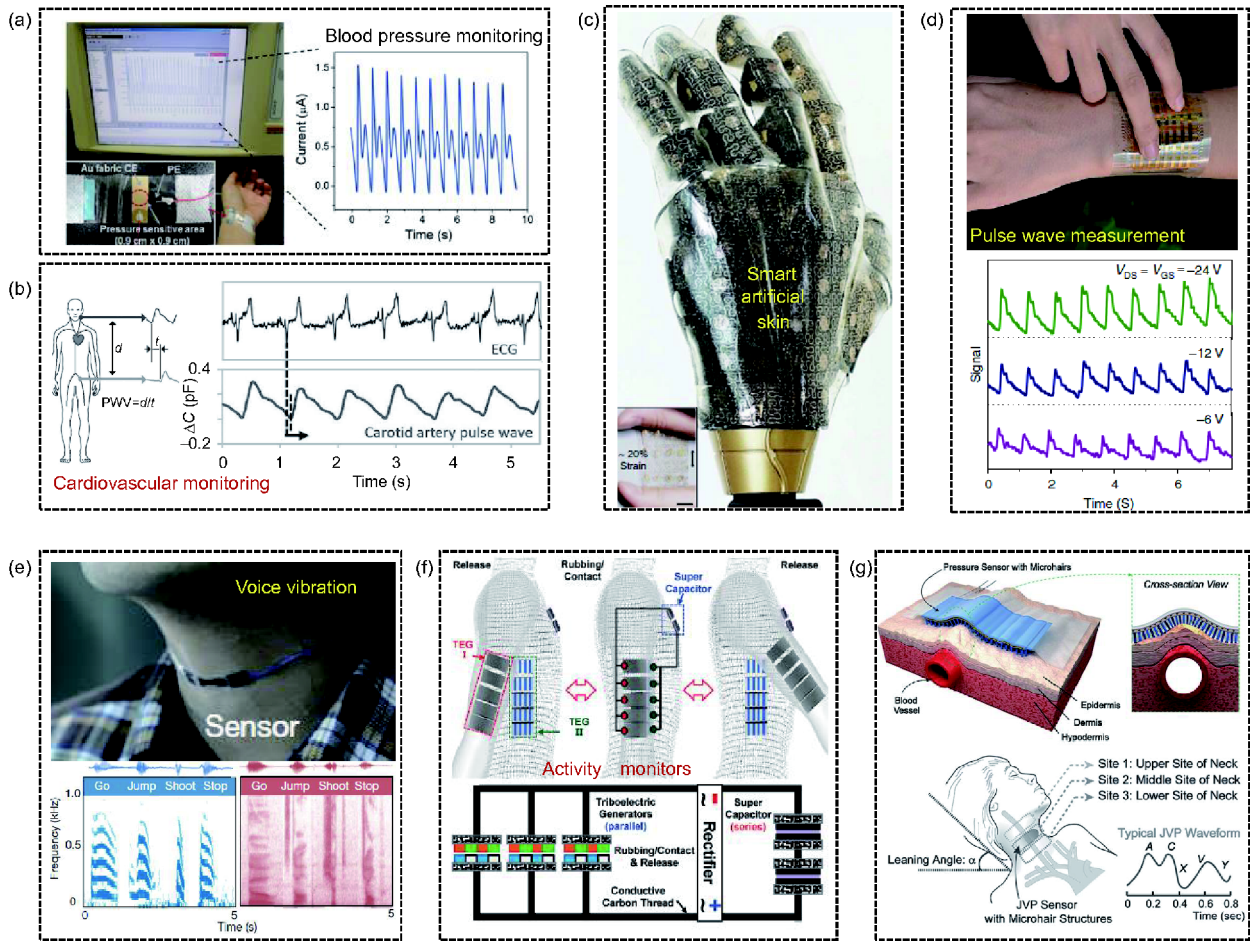

Figure 6 (Color online) Some promising applications of pressure sensors. (a) Demonstration of blood pressure monitoring using a pressure sensor [60]; (b) real-time transient signals of pulse-wave velocity recorded at the femoral and carotid artery [61]; (c) photograph of a representative smart artificial skin with integrated stretchable sensors and actuators [62]; (d) sensors attached to the artery of the wrist and the signals [63]; (e) a sensor attached to the neck for recording human speech [64]; (f) schematic descriptions and the morphology of integrated energy devices [65]; (g) measurement of pulses on the identical contact sites of the neck [66].

textile electrodes for biosignal acquisition specifically in cardiac monitoring [78], as shown in Figure 7(d). The device with new graphene-clad textile electrodes has excellent conformity as compared with conventional electrodes.

Commercial device-level flexible electronic devices have also been proposed for ECG measurements. An epidermal carbon nanotube electronic device was fabricated to robustly record ECG signals [79], as shown in Figure 8(a). The self-adhesive electrode of the device maintains an excellent conformal contact even on wrinkled skin, and this electrode can also be used to record various other bioelectrical signals without damaging the skin. Despite significant progress in the fabrication of flexible biosensors that naturally comply with the epidermis, the rich chemical information has often been neglected. As shown in Figure 8(b), researchers have introduced a hybrid sensing system that offers simultaneous real-time monitoring of the lactate and ECG signals [80]. The ECG signals were quite different between the cases with and without sweat. Figure 8(c) shows a single wave recorded in the apex cardiogram that identified various peaks [81]. The measurements showed excellent signal-to-noise ratio, reproducibility, and stability. Furthermore, a wearable sensor patch has been fabricated by using a process flow compatible with the method of flexible printed circuit boards; this patch consisted of inkjet-printed gold ECG electrodes and a stencil-printed nickel oxide thermistor [82].

In addition to ECG monitoring, other bioelectrical signals, such as EEG, EOG, and EMS, also play an important role in medical diagnosis and daily health monitoring [83,84]. In particular, researchers have reported an epidermal device that can achieve conformal contact with the skin and adhere well to the skin using only van der Waals interactions [85], as shown in Figure 9(a); this epidermal device presents the spectrogram of the alpha rhythm and the eye opening and blinking using the EEG data. Recently, a patchable sensor has been fabricated; it consists of three electrodes, including a measurement electrode, a ground electrode, and a reference electrode [86], as shown in Figure 9(b). This sensor records the EOG signals of three types of eye movements: blinking, looking upward, and looking downward. Moreover, certain

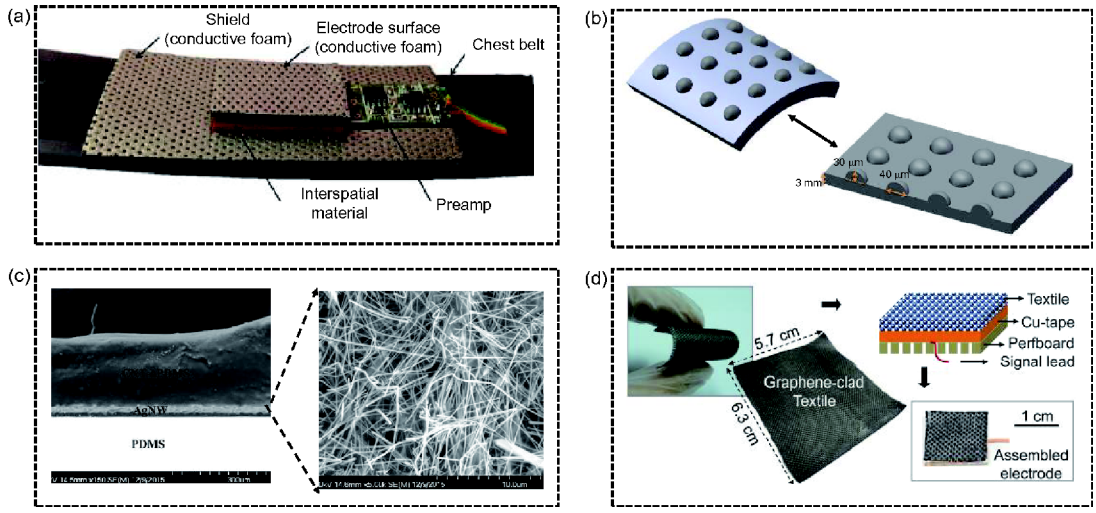

Figure 7 (Color online) Micrographs of various flexible electrodes in ECG devices. (a) Structural details with conductive foam [75]; (b) dome array on the electrode [76]; (c) three-layered structure of composite electrode and the SEM image of the middle layer (AgNWs) [77]; (d) a new graphene-coated textile electrode [78].

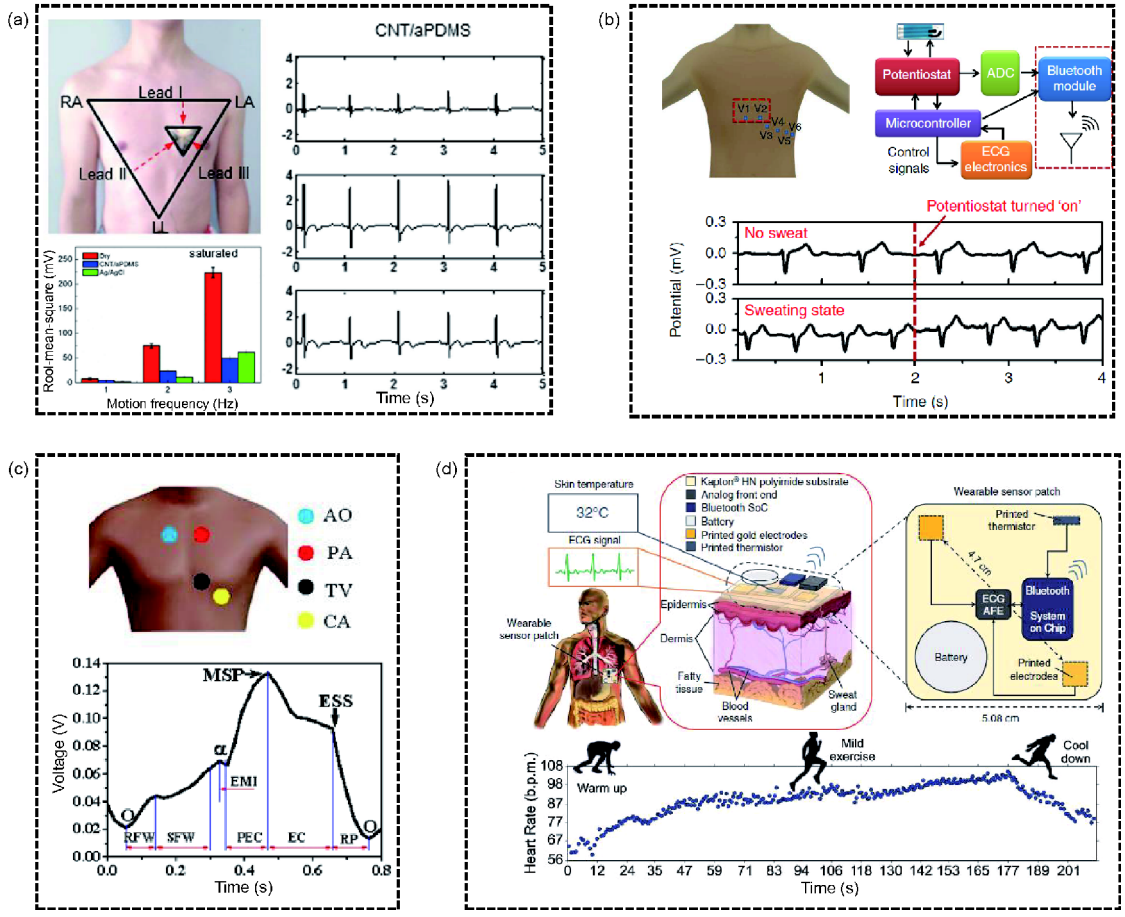

Figure 8 (Color online) Typical commercial device-level flexible ECG measurement equipment. (a) ECG waveforms recorded by the device with CNT electrodes [79]; (b) effect of amperometric measurement on the ECG signals with and without sweat [80]; (c) apex cardiogram recording [81]; (d) flexible hybrid electronics and the heart rate during exercise [82].

studies have reported flexible electronic systems for measuring the EMG signal. As shown in Figure 9(c), Xu et al. [87] reported an EMG system that consisted of multiple transcutaneous electrical stimulation electrodes integrated on a common substrate. The evaluations of EMG signals under four conditions were further carried out by this device. Another surface EMG sensor has also been reported [88] in which the thickness of elastomer membrane substrates was

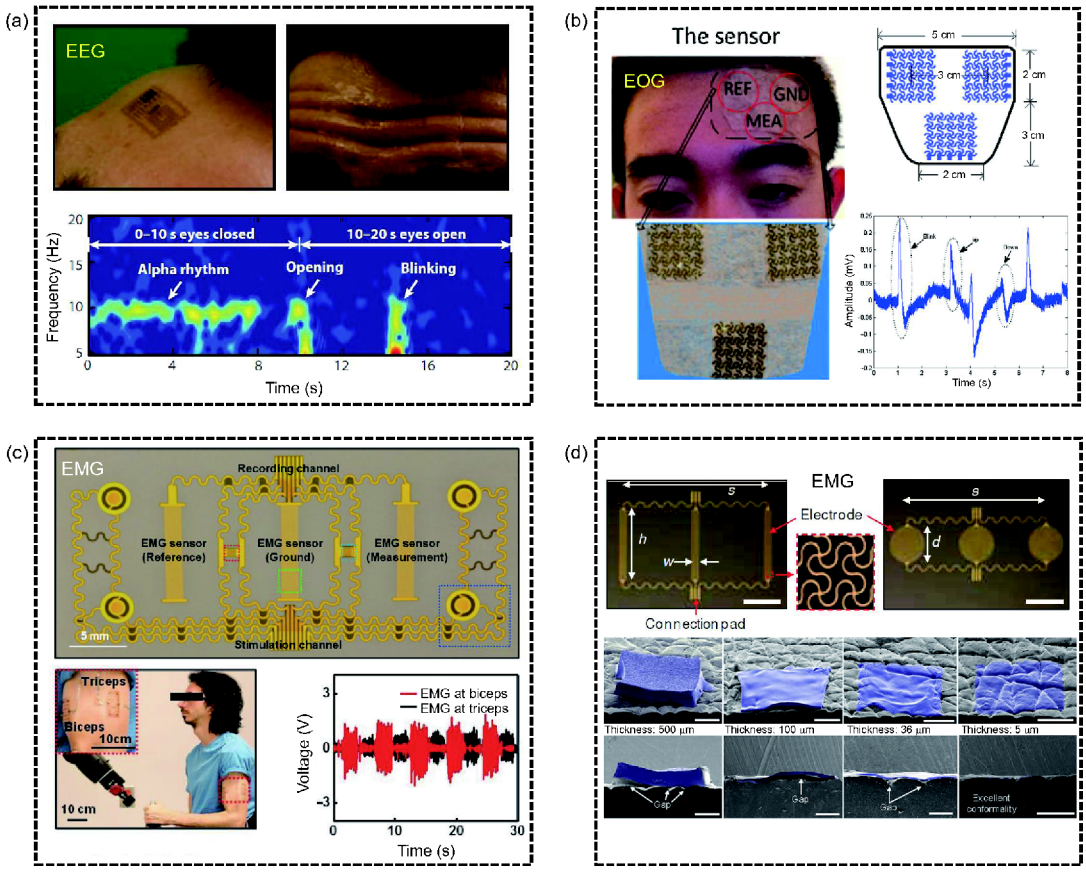

Figure 9 (Color online) (a) EEG measurement corresponding to eye opening and blinking [85]; (b) flexible EOG systems and signals recording [86]; (c) skin-like sensors and EMG signals [87]; (d) structure of the surface EMG sensor and the degree of conformal contact with different thicknesses of elastomers [88].

systematically studied to assess the degree of conformal contact, as shown in Figure 9(d).

2.4 Respiratory monitoring

In the past decade, various respiratory diseases, such as the sleep apnea syndrome, asthma, and chronic obstructive pulmonary diseases, have caused substantial problems to human health. Most respiratory diseases are chronic in nature and have a major impact on both the individual patients and the community. Information about the respiratory state is of great significance in several medical applications. In real life, most respiratory monitoring devices are designed to achieve long-term signal monitoring and disease diagnosis by integrating the various basic sensors mentioned above [89].

Many integrated electronic devices for respiratory monitoring have also been reported [90-92]. In particular, a flexible projected capacitive sensing mattress composed of a multielectrode sensor array has been proposed for personal health assessment [93], as shown in Figure 10(a). Compared with the conventional respiratory monitoring system, this device can identify human gestures and motions during sleep. Respiratory flow is another physiological indicator and is usually measured by using the nasal cannula. To noninvasively monitor respiratory flow in real time, a flexible flow sensor has been fabricated, which monolithically integrates four resistors of a Wheatstone bridge [94] (see Figure 10(b)). Experiments were further conducted to verify the feasibility and effectiveness of monitoring and diagnosing respiratory diseases. Recently, a wearable self-powered active sensor based on a flexible piezoelectric nanogenerator has been fabricated [95]; the structural details of this sensors are given in Figure 10(c). The self-powered sensor can be used to monitor human respiration, subtle muscle movements, and voice recognition devices. The electrical output signals exhibit good reliability and feasibility. Moreover, the respiratory symptoms can also be monitored, such as airflow, snoring, end-tidal CO_2, esophageal pressure, and breathing humidity [96,97]. It has become increasingly important to have wireless, non-invasive flexible devices for monitoring the real-time respiratory process; this provides sufficient information for early detection and diagnosis of diseases [98-100].

2.5 Hydration monitoring

Skin hydration, which is another important indicator for analyzing diseases, can be characterized by measuring

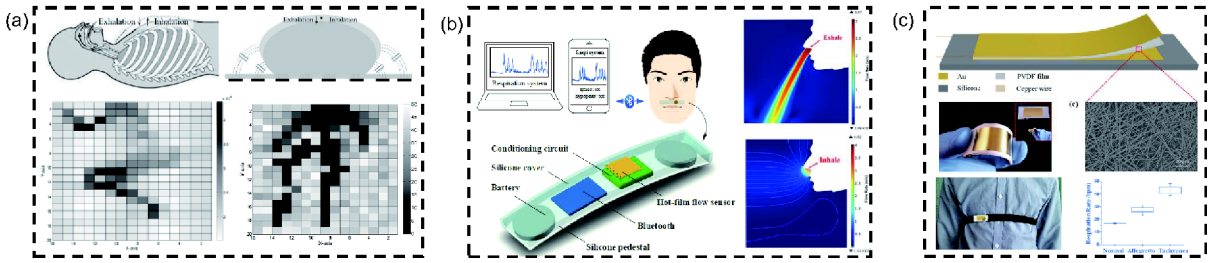

Figure 10 (Color online) Various respiratory monitoring devices and sensors. (a) Thoracic volume variation during respiration and gesture recognition during sleep [93]; (b) schematic of the flow sensor and the simulated exhalation and inhalation processes [94]; (c) piezoelectric active sensor and the measurement of respiration rate [95].

thermal conductivity [101,102], electrical impedance [103,104], or millimeter wave reflection [105], as illustrated in Figure 11. Traditional skin hydration sensors rely on capacitive measurements or impedance-based measurements in which the mechanical force is generally applied to a rigid electrode. The force compresses and deforms the skin thereby altering the capacitive properties and the hydration characteristics. To measure skin hydration, electrical impedance provides the most reliable assessment. The basic principle of the impedance method is to bridge the correlations between the electrical parameters of biological tissues and their water content [106]. For example, an embedded piezoresistive microcantilever sensor has been developed to measure the saliva osmolality and to provide the appropriate hydration level in the human body [107]. The same measurement principle was used subsequently in ref. [108].

Typical epidermal sensors for conformal skin hydration monitoring are shown in Figure 12. Huang et al. [109] presented an epidermal sensor for conformal skin hydration monitoring by performing impedance measurements, as illustrated in Figure 12(a). Their skin hydration sensor consisted of pairs of electrodes that formed eight measurement channels. Four of them contacted the skin directly and measured the skin impedance, and another four channels were insulated by thin dielectric layers as the reference electrodes. The reversible and soft contact of the device with the skin ensured that the measurements were accurate and repeatable. The epidermal electronic sensor adhered very well to the various epidermises having different surface morphologies by using only van der Waals forces. Zhou et al. [110] fabricated a gold nanoparticle-based colorimetric sensor to distinguish between dehydration and over-hydration using easily observable color changes, which were based on the principle that the gold nanoparticles allow colorimetric detection; the color of gold nanoparticles changes because of colloidal stability.

Figure 12(b) shows a wireless hydration sensor relying on passive inductive coupling proposed by ref. [111]. This multimodal epidermal electronic sensor contains a miniaturized array of impedance-measurement electrodes that enable the calibrated conversion of electrical quantities to hydration levels. The wireless methodology provides a convenient strategy for epidermal sensing devices that do not use power supplies or active components. Researchers have fabricated and tested another wireless sensor in the form of a capacitor [112], as shown in Figure 12(c). In ref. [112], the capacitor component contains two parallel electrodes made of silver nanowires in a polydimethylsiloxane matrix that allows conformal contact with the skin. This hydration sensor is insensitive to the external changes in humidity and exhibits good stability in skin hydration monitoring. In addition, Krishnan et al. [113] fabricated a multimodal sensor that integrated the thermal and electrical characterization capabilities into a single platform; this sensor provided improved insights into the state of hydration (see Figure 12(d)). To better design and optimize the epidermal hydration sensing system (Figure 12(e)), an analytical model for the concentric coplanar capacitor was proposed to determine the capacitance and impedance in terms of the material and geometric parameters [114]. The systems mentioned above can provide noninvasive, wearable, and wireless signal monitoring and transmission, which have application potentials in the evaluation of athletic performance, diagnosis of skin diseases, and so on.

2.6 Sweat monitoring

To obtain more insightful information regarding human physiological indicators, various conformal chemical biosensors have been developed to noninvasively monitor biomarkers in human body fluids [115-117]. Many types of fluid biomarkers have been used as indicators for disease detection. For example, examining the cerebrospinal fluid [118] can be useful for detecting the first onset of psychosis signature. Saliva [119,120] is a readily available medium to be explored for health and disease surveillance. Scientific data has established the diagnostic value of saliva to detect diseases. However, persistent real-time disease surveillance requires continuous access to body fluids. Sweat, which contains tens to hundreds of compounds, plays a major role in the analysis of specific electrolyte concentrations. Various metal ions and biomolecules that accumulate inside the hu-

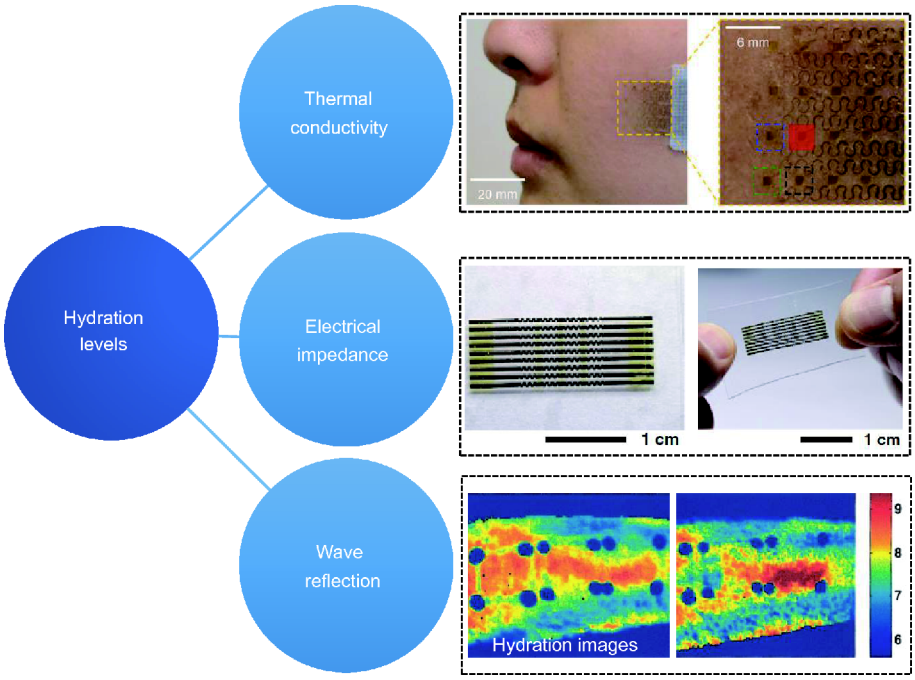

Figure 11 (Color online) Typical methods for measuring skin hydration.

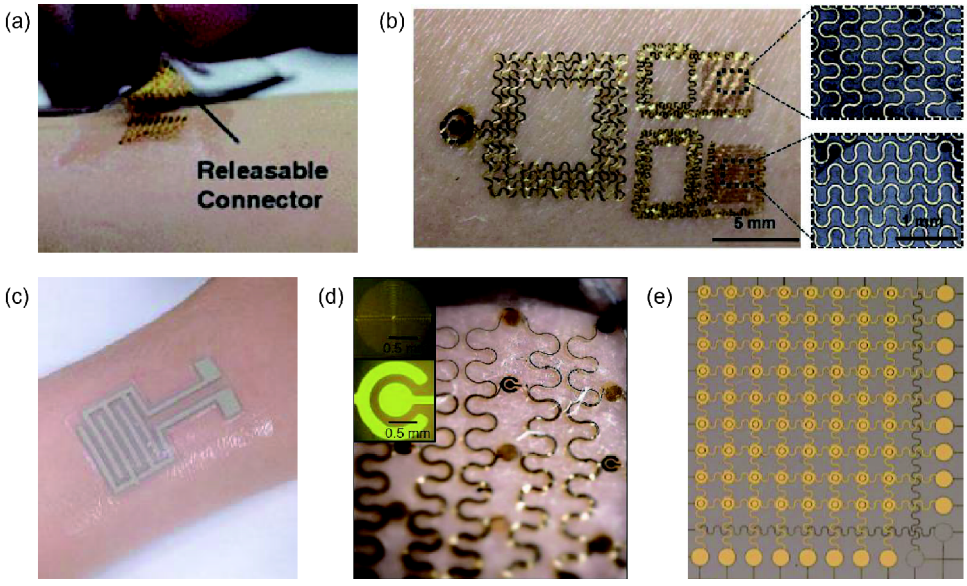

Figure 12 (Color online) Typical epidermal sensors for conformal skin hydration monitoring. (a) Soft, releasable connectors between the hydration sensors and the skin [109]; (b) a sensor integrated directly on the skin [111]; (c) photograph showing the AgNW sensor placed on the inner side of the forearm [112]; (d) sensor array for epidermal hydration mapping [113]; (e) optical micrograph of an epidermal hydration sensing system [114].

man body can be monitored in sweat, including sodium [121,122], ammonium [123], lactate [124,125], chloride [126], and glucose [127]; these molecules and ions are closely related to human health conditions. For instance, the excessive loss of Na^+ or K^+ can result in hypokalemia, hyponatremia, or muscle cramps, and the accumulation of excess copper can lead to Wilson's disease and kidney failure [128]. Sweat lactate has been reported to be metabolically related to pressure ischaemia [129]. Despite all these, it is still a great challenge to detect the heavy metals in sweat because of their extremely low concentration of the order of μg/L.

Numerous flexible platforms of sweat biosensors have been proposed and developed based on different detection strategies in the past decade, as illustrated in Figure 13. Sweat analysis is commonly performed by using a sweat collector that is directly attached to the human body during physical exercise [130]. The sweat is then extracted from the

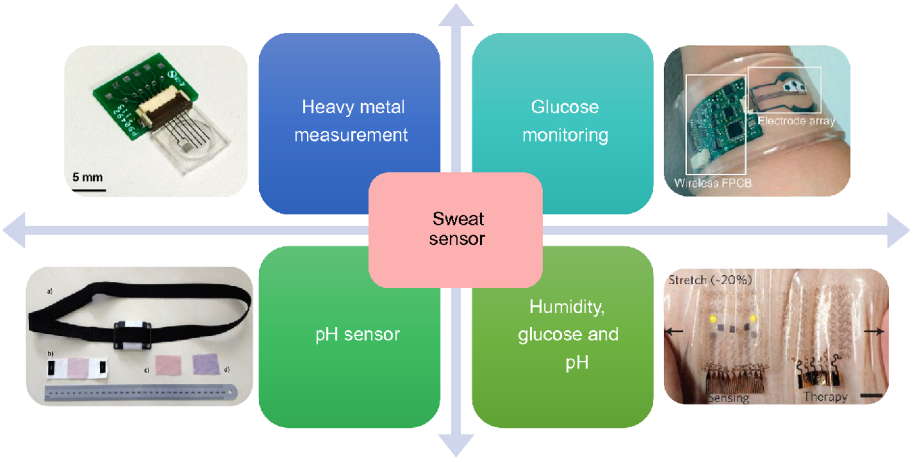

Figure 13 (Color online) Measurement principles for sweat monitoring.

collector and analyzed by various selective sensors. Device-level demonstrations are provided by using various physiological indicators, such as sweat loss, pH value, and sweat rate, along with various biomarkers, such as lactate, glucose, chloride, and creatinine. In particular, a soft wearable microfluidic system that enables precise and routine measurements of secretory fluidic pressures has been fabricated [131]; the magnitudes of these pressures can provide insights into the physiological health and the psychological stress factors. A soft and thin sweat monitoring device was also designed to store sweat and calculate the sweat rate by introducing a microfluidic network with capillary bursting valves [132]. A wearable and non-toxic pH sensor has been fabricated to bridge the connection between the sweat pH and sodium concentration [133]; this was an optical pH sensor having several advantages as compared with the classical impedance-based sensors for sweat conductivity monitoring [134]. Moreover, Lee et al. [135] fabricated a graphene biochemical sensor with Ag/AgCl counter electrodes; this sensor showed excellent sensitivity and selectivity in monitoring the various biomarkers in human sweat.

To obtain more insightful information regarding human health conditions, different research groups tried to develop multiplexed sensing in human sweat samples based on biosensor arrays. As shown in Figure 14(a), Gao et al. [136] developed a fully integrated wearable sensor array to measure the detailed sweat profile of human subjects. The skin-conforming plastic-based device had high repeatability and excellent stability for the selective detection of multiple heavy metals, such as Zn, Cd, Pb, Cu, and Hg. The device contained five sensors and more than ten chips (see Figure 14(b)), which could measure and accurately assess multiplexed signals in sweat via signal processing of the physiological state of the human subjects. Another wearable sweat analysis platform was developed to extract sufficient sweat for robust monitoring using an electrochemically enhanced iontophoresis interface [137], as shown in Figure 14(c). This platform enabled a real-time assessment of heavy metals present in sweat, such as Zn, Cd, Pb, Cu, and Hg and gave early warnings of heavy metal exposure. Furthermore, as shown in Figure 14(d), Huang et al. [138] introduced a material and design strategy to integrate flexible and stretchable wireless sensors on the functional elastomeric substrates for the epidermal analysis of sweat; the colorimetric responses to the pH values and concentrations of various ions (OH^-, H^+, Cu^+, and Fe^{2+}) provided the capabilities relevant to sweat analysis. This platform provides a strategy to develop sensors for monitoring a range of parameters associated with sweat and other human body fluids. From the above description, we can see that sweat monitoring enables the real-time assessment of the physiological state of subjects and can provide various profiles of human subjects who are engaged in prolonged outdoor and indoor activities.

2.7 Other multiplexed monitoring

Generally, human lesions are accompanied by changes in multiple physiological indicators. To improve the accuracy of human physiological signals, multisignal monitoring is being developed. In addition to the physiological signal indicators mentioned in the previous section, blood oxygen, blood glucose, and pulse are also important signals. Using a comprehensive analysis of different signals [139-141], we can obtain more accurate physiological information. Recently, a multimodal sweat-based glucose monitoring device has been developed based on the integration of pH, temperature, and humidity measurements; this maximized the accuracy of the sensing [142], as shown in Figure 15(a). A flexible microfluidic platform with fully integrated metabolites, electrolytes, and temperature sensors has also been reported [143]. This device provides continuous and si-

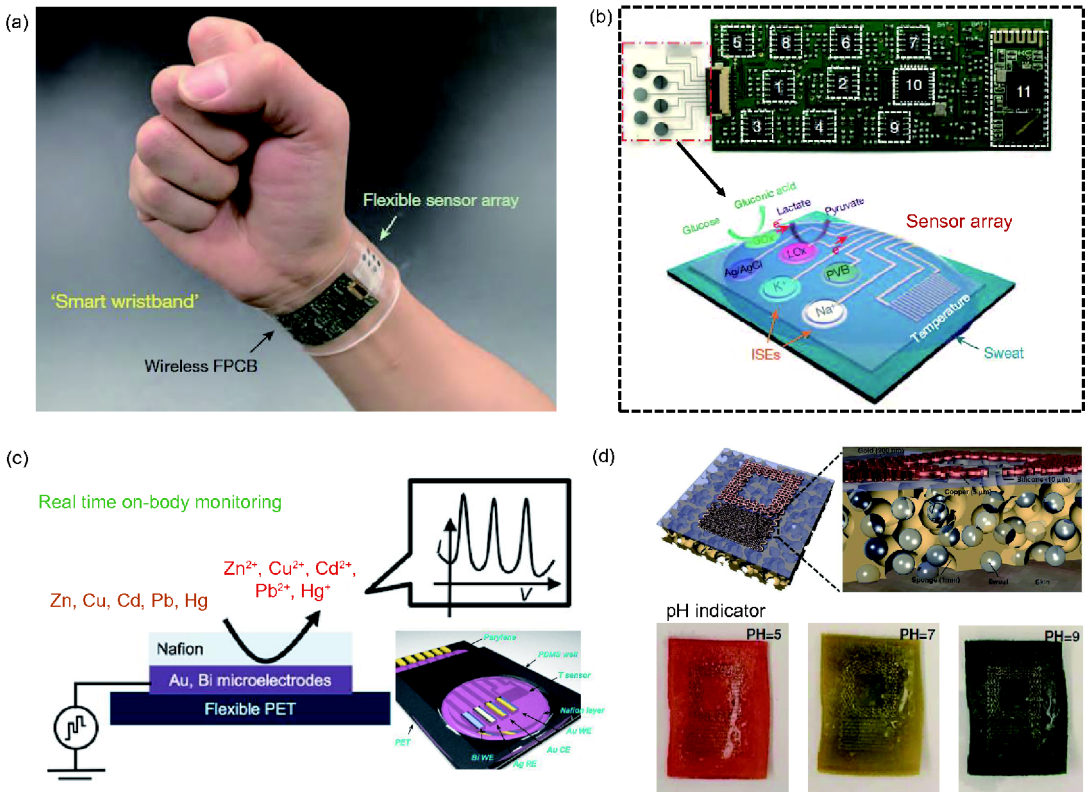

Figure 14 (Color online) (a) Photograph of a wearable device integrating the multiplexed sensor array; (b) flattened flexible device and sensor array [136]; (c) schematic showing the simultaneous multiplexed monitoring of heavy metals [137]; (d) schematic illustration of a passive wireless capacitive sensor and the series of pictures of a sensor doped with a pH indicator [138].

multaneous measurement of temperature and sweat metabolites including lactate and sodium, and it transmits the information wirelessly. The schematic of this platform as well as the monitored signals is shown in Figure 15(b).

Material selection plays an important role in the preparation of multifunctional monitoring sensors. By integrating the uniform free-standing ultrathin film of single-walled carbon nanotubes, Wang et al. [144] fabricated flexible e-skins that can simultaneously monitor wrist pulse and muscle movement. This sensing device demonstrated high performance with superior sensitivity and very low detectable pressure limit. Furthermore, Gao et al. [145] fabricated a liquid metal-based pressure sensor that achieved an excellent pressure detection resolution (sub –100 Pa). This sensor provided excellent thermal stability in the range of 20°C-50°C through temperature self-compensation. As shown in Figure 16 (a), the real-time monitoring of pulse and various gestures, such as touching or holding objects, were also demonstrated by the multiple embedded sensors. Almost simultaneously, materials and device concepts for multifunctional flexible platforms have been reported [146]. Wearable biosensors based on the optoelectronic functionality can emit infrared and red light and backscatter from or transmit through living tissues. Multifunctional flexible platforms provided wireless capture and transmission of photoplethysmograms, including the information on blood oxygenation, heart rate, and heat-rate variability, as shown in Figure 16(b). In addition, a wearable multiplexed force touch sensor array has been fabricated by using the epoxy-copper-ITO multilayer electrodes [147], as illustrated in Figure 16(c). Wireless drone control has also been performed by using touch and pressure sensors.

Specially designed sensors can be integrated on a bio-absorbable substrate to produce transient electronics [148-150]. These electronic devices are of great significance for medical implants and environmental monitors because they are designed to be partially or fully dissolvable in ambient environment with controlled and predictable kinetics at predefined time scales [151]. These implantable biomedical components are always used within or on the body surface; flexibility is very significant to avoid the discomfort caused by incongruity with the deformation of the organ surface. The tensile stiffness, bending stiffness, elongation, and other mechanical properties of these devices need to be less than or comparable to those of the human body organs. A series of in vivo experiments further demonstrated that the transient devices implanted in the subdermal region of mice can be completely degraded after three weeks without inducing significant inflammatory reactions. The most advanced biocompatible devices use thin films of either zinc oxide

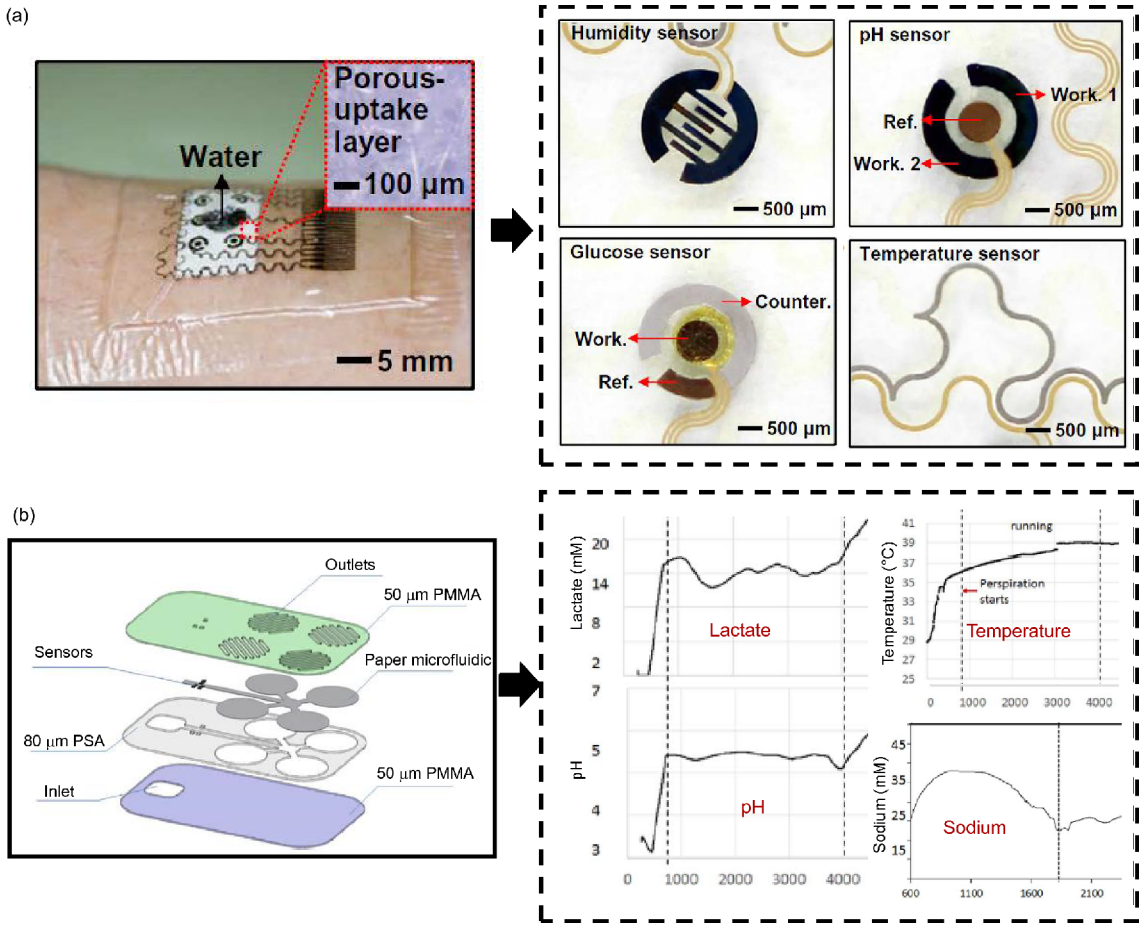

Figure 15 (Color online) (a) Optical image of the wearable sweat analysis patch and the characterization of individual sensors [142]; (b) schematic of the fabrication steps of the microfluidic chip and changes in location, temperature, pH, and sodium measurements [143].

(ZnO) [152] or single crystalline silicon nanomembranes [153,154]. For conductors, metals and metal alloys [155] are used; for substrates, polymers and metal foils are used. Using a transient electronic device, the researchers integrated the diagnostic and therapeutic stretchable sensor that could measure and map the temperature and electrophysiological signals [156]. Recently, another fully decomposable and biocompatible semiconducting polymer and totally disintegrable flexible circuit has been demonstrated [157] (see Figure 16(d)). These multifunctional sensors were fabricated on a thin and bioresorbable sheet of silk to achieve a transient effect in the organism. The material layouts and mechanical formats provide a wide range of design space and application scenario for implantable biocompatible devices.

Multisensor-integrated flexible electronic devices are gaining increasing importance in the human healthcare sector. It is very important to coordinate various functional components for the acquisition of stable and reliable physiology signals. The integration level of the sensors will improve by including multiple-information fusion and sensor standardization, which will significantly improve the convenience, dependability, and utility efficiency of the flexible electronics used for healthcare monitoring.

3 Conclusion

Flexible electronics have great potential applications in the human healthcare sector. Current studies have mostly investigated materials, fundamental mechanics, fabrication technologies, electronic informatics, and the functional components for signal monitoring. This paper reviews the applications used for monitoring various signals for human healthcare, including temperature, pressure, sweat, bioelectricity, hydration, etc. Many of the devices remain effective only in controlled, laboratory settings, and immediate industrial applications and some fundamental mechanisms are still lacking. Numerous opportunities and challenges remain for future research and development of high-performance sensors in the field of human healthcare. Human tissue lesions are always accompanied by a variety of physiological signal changes; therefore, high-precision multiplexed signal monitoring and processing technologies have become extremely important in the design of biosensors. With an improved understanding of biosensors and the architectures of

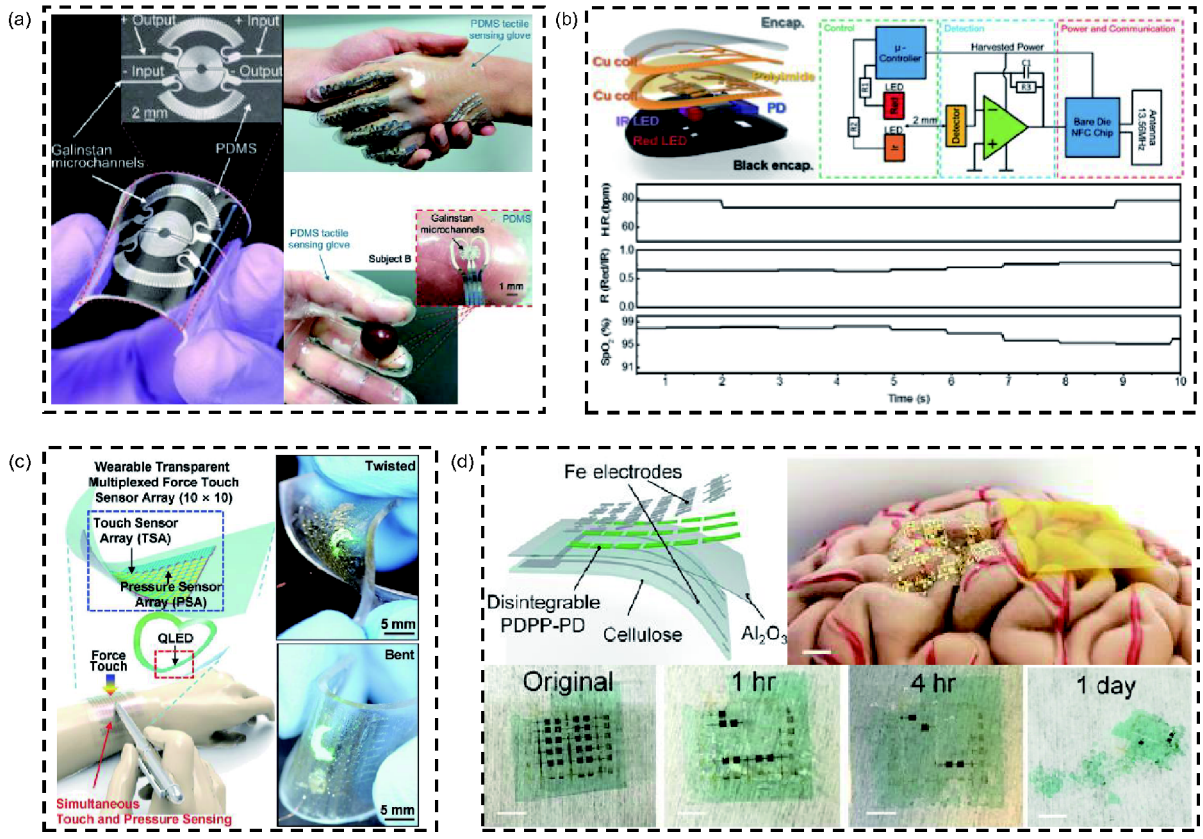

Figure 16 (Color online) (a) A liquid metal-based pressure sensor and the gesture recognition [145]; (b) multifunctional flexible platform and various signal measurements [146]; (c) a transparent and wearable force touch sensor array and its deformability [147]; (d) disintegrable electronics with different stages of disintegration [157].

flexible and stretchable electronic devices, it will be possible to develop more functional and powerful integrated electronic systems. This will improve public health by bringing about revolutionary changes in long-term health monitoring devices.

This work was supported by the National Natural Science Foundation of China (Grant Nos. 11572323, 11772331, and 11302038), the Chinese Academy of Sciences via the "Hundred Talent Program", the Strategic Priority Research Program of the Chinese Academy of Sciences (Grant No. XDB22040501), the State Key Laboratory of Structural Analysis for Industrial Equipment, Dalian University of Technology (Grant No. GZ1603), the State Key Laboratory of Digital Manufacturing Equipment and Technology, Huazhong University of Science and Technology (Grant No. DMETKF2017008), and the Young Elite Scientists Sponsorship Program by China Association for Science and Technology (CAST) (Grant No. 2015QNRC001).

1 X. Xu, M. Davanco, X. Qi, and S. R. Forrest, Org. Electron. **9**, 1122 (2008).
2 I. Jung, G. Shin, V. Malyarchuk, J. S. Ha, and J. A. Rogers, Appl. Phys. Lett. **96**, 021110 (2010).
3 S. Wagner, S. P. Lacour, J. Jones, P. I. Hsu, J. C. Sturm, T. Li, and Z. Suo, Phys. E-Low-dimensional Syst. NanoStruct. **25**, 326 (2004).
4 M. L. Hammock, A. Chortos, B. C. K. Tee, J. B. H. Tok, and Z. Bao, Adv. Mater. **25**, 5997 (2013).
5 D. H. Kim, S. Wang, H. Keum, R. Ghaffari, Y. S. Kim, H. Tao, B. Panilaitis, M. Li, Z. Kang, F. Omenetto, Y. Huang, and J. A. Rogers, Small **8**, 3263 (2012).
6 T. Song, H. Cheng, H. Choi, J. H. Lee, H. Han, D. H. Lee, D. S. Yoo, M. S. Kwon, J. M. Choi, S. G. Doo, H. Chang, J. Xiao, Y. Huang, W. I. Park, Y. C. Chung, H. Kim, J. A. Rogers, and U. Paik, ACS Nano **6**, 303 (2012).
7 *Biosensors Market (Electrochemical, Optical, Piezoelectric & Thermistor)—Global Industry Analysis, Size, Share, Growth, Trends and Forecast, 2012-2018*, Market Report (Transparency Market Research, 2013).
8 S. R. Forrest, Nature **428**, 911 (2004).
9 H. Kim, E. Brueckner, J. Song, Y. Li, S. Kim, C. Lu, J. Sulkin, K. Choquette, Y. Huang, R. G. Nuzzo, and J. A. Rogers, Proc. Natl. Acad. Sci. USA **108**, 10072 (2011).
10 Q. Ma, and Y. Zhang, J. Appl. Mech. **83**, 111008 (2016).
11 Y. Su, Z. Liu, S. Kim, J. Wu, Y. Huang, and J. A. Rogers, Int. J. Solids Struct. **49**, 3416 (2012).
12 Y. Su, S. Wang, Y. A. Huang, H. Luan, W. Dong, J. A. Fan, Q. Yang, J. A. Rogers, and Y. Huang, Small **11**, 367 (2015).
13 H. Liu, R. Y. Xue, X. C. Ping, J. Q. Hu, H. P. Wu, H. Zhang, X. Guo, R. Li, Y. L. Chen, and Y. W. Su, Sci. China-Phys. Mech. Astron. 2018, doi: 10.1007/s11433-018-9238-2.
14 C. Pailler-Mattei, S. Bec, and H. Zahouani, Med. Eng. Phys. **30**, 599 (2008).
15 M. Kaltenbrunner, T. Sekitani, J. Reeder, T. Yokota, K. Kuribara, T. Tokuhara, M. Drack, R. Schwödiauer, I. Graz, S. Bauer-Gogonea, S. Bauer, and T. Someya, Nature **499**, 458 (2013).
16 D. H. Kim, J. Viventi, J. J. Amsden, J. Xiao, L. Vigeland, Y. S. Kim, J. A. Blanco, B. Panilaitis, E. S. Frechette, D. Contreras, D. L. Kaplan, F. G. Omenetto, Y. Huang, K. C. Hwang, M. R. Zakin, B. Litt,

and J. A. Rogers, Nat. Mater **9**, 511 (2010).
17 H. Araki, J. Kim, S. Zhang, A. Banks, K. E. Crawford, X. Sheng, P. Gutruf, Y. Shi, R. M. Pielak, and J. A. Rogers, Adv. Funct. Mater. **27**, 1604465 (2017).
18 K. H. Choi, M. Zubair, and H. W. Dang, Jpn. J. Appl. Phys. **53**, 05HB02 (2014).
19 C. Y. Lee, C. H. Lin, and Y. M. Lo, Sensors **11**, 3706 (2011).
20 Q. Tan, Z. Ren, T. Cai, C. Li, T. Zheng, S. Li, and J. Xiong, J. Sens. **2015**, 1 (2015).
21 E. Chiappini, S. Sollai, R. Longhi, L. Morandini, A. Laghi, C. E. Osio, M. Persiani, S. Lonati, R. Picchi, F. Bonsignori, F. Mannelli, L. Galli, and M. de Martino, J. Clinical Nursing **20**, 1311 (2011).
22 T. Q. Trung, S. Ramasundaram, B. U. Hwang, and N. E. Lee, Adv. Mater. **28**, 502 (2016).
23 L. Tian, Y. Li, R. C. Webb, S. Krishnan, Z. Bian, J. Song, X. Ning, K. Crawford, J. Kurniawan, A. Bonifas, J. Ma, Y. Liu, X. Xie, J. Chen, Y. Liu, Z. Shi, T. Wu, R. Ning, D. Li, S. Sinha, D. G. Cahill, Y. Huang, and J. A. Rogers, Adv. Funct. Mater. **27**, 1701282 (2017).
24 R. C. Webb, A. P. Bonifas, A. Behnaz, Y. Zhang, K. J. Yu, H. Cheng, M. Shi, Z. Bian, Z. Liu, Y. S. Kim, W. H. Yeo, J. S. Park, J. Song, Y. Li, Y. Huang, A. M. Gorbach, and J. A. Rogers, Nat. Mater. **12**, 938 (2013).
25 Y. Chen, B. Lu, Y. Chen, and X. Feng, Sci. Rep. **5**, 11505 (2015).
26 Y. Zhang, R. Chad Webb, H. Luo, Y. Xue, J. Kurniawan, N. H. Cho, S. Krishnan, Y. Li, Y. Huang, and J. A. Rogers, Adv. Healthcare Mater. **5**, 119 (2016).
27 Z. Wu, C. Li, J. Hartings, S. Ghosh, R. Narayan, and C. Ahn, J. Micromech. Microeng. **27**, 025001 (2017).
28 I. Graz, M. Krause, S. Bauer-Gogonea, S. Bauer, S. P. Lacour, B. Ploss, M. Zirkl, B. Stadlober, and S. Wagner, J. Appl. Phys. **106**, 034503 (2009).
29 S. K. Mahadeva, S. Yun, and J. Kim, Sens.s Actuators A-Phys. **165**, 194 (2011).
30 J. Yang, D. Wei, L. Tang, X. Song, W. Luo, J. Chu, T. Gao, H. Shi, and C. Du, RSC Adv. **5**, 25609 (2015).
31 W. P. Shih, L. C. Tsao, C. W. Lee, M. Y. Cheng, C. Chang, Y. J. Yang, and K. C. Fan, Sensors **10**, 3597 (2010).
32 T. Yokota, Y. Inoue, Y. Terakawa, J. Reeder, M. Kaltenbrunner, T. Ware, K. Yang, K. Mabuchi, T. Murakawa, M. Sekino, W. Voit, T. Sekitani, and T. Someya, Proc. Natl. Acad. Sci. USA **112**, 14533 (2015).
33 A. Koh, S. R. Gutbrod, J. D. Meyers, C. Lu, R. C. Webb, G. Shin, Y. Li, S. K. Kang, Y. Huang, I. R. Efimov, and J. A. Rogers, Adv. Healthcare Mater. **5**, 373 (2016).
34 X. Ren, K. Pei, B. Peng, Z. Zhang, Z. Wang, X. Wang, and P. K. L. Chan, Adv. Mater. **28**, 4832 (2016).
35 X. Wang, L. Dong, H. Zhang, R. Yu, C. Pan, and Z. L. Wang, Adv. Sci. **2**, 1500169 (2015).
36 Y. Zang, F. Zhang, C. Di, and D. Zhu, Mater. Horiz. **2**, 140 (2015).
37 J. M. Cannata, D. Vilkomerson, T. Chilipka, H. C. Yang, S. Han, V. L. Rowe, and F. A. Weaver, J. Acoust. Soc. Am. **128**, 2304 (2010).
38 A. T. Sepúlveda, F. Fachin, R. G. Villoria, B. L. Wardle, J. C. Viana, A. J. Pontes, and L. A. Rocha, Procedia Eng. **25**, 140 (2011).
39 K. F. Lei, K. F. Lee, and M. Y. Lee, MicroElectron. Eng. **99**, 1 (2012).
40 H. C. Lim, B. Schulkin, M. J. Pulickal, S. Liu, R. Petrova, G. Thomas, S. Wagner, K. Sidhu, and J. F. Federici, Sens. Actuators A-Phys. **119**, 332 (2005).
41 C. X. Liu, and J. W. Choi, Microsyst. Technol. **18**, 365 (2011).
42 X. Liu, Y. Zhu, M. W. Nomani, X. Wen, T. Y. Hsia, and G. Koley, J. Micromech. Microeng. **23**, 025022 (2013).
43 B. R. Burg, T. Helbling, C. Hierold, and D. Poulikakos, J. Appl. Phys. **109**, 064310 (2011).
44 M. Akiyama, Y. Morofuji, T. Kamohara, K. Nishikubo, M. Tsubai, O. Fukuda, and N. Ueno, J. Appl. Phys. **100**, 114318 (2006).
45 W. Choi, J. Lee, Y. Kyoung Yoo, S. Kang, J. Kim, and J. Hoon Lee, Appl. Phys. Lett. **104**, 123701 (2014).
46 A. T. Sepúlveda, R. G. D. Villoria, J. C. Viana, A. J. Pontes, B. L. Wardle, and L. A. Rocha, Procedia Eng. **47**, 1177 (2012).
47 C. Dagdeviren, Y. Su, P. Joe, R. Yona, Y. Liu, Y. S. Kim, Y. A. Huang, A. R. Damadoran, J. Xia, L. W. Martin, Y. Huang, and J. A. Rogers, Nat. Commun. **5**, 4496 (2014).
48 J. H. Cho, S. H. Ha, and J. M. Kim, Nanotechnology **29**, 155501 (2018).
49 Y. Jiang, Z. Liu, N. Matsuhisa, D. Qi, W. R. Leow, H. Yang, J. Yu, G. Chen, Y. Liu, C. Wan, Z. Liu, and X. Chen, Adv. Mater. **30**, 1706589 (2018).
50 M. Y. Cheng, X. H. Huang, C. W. Ma, and Y. J. Yang, J. Micromech. Microeng. **19**, 115001 (2009).
51 M. Leineweber, G. Pelz, M. Schmidt, H. Kappert, and G. Zimmer, Sens. Actuators A-Phys. **84**, 236 (2000).
52 S. C. B. Mannsfeld, B. C. K. Tee, R. M. Stoltenberg, C. V. H. H. Chen, S. Barman, B. V. O. Muir, A. N. Sokolov, C. Reese, and Z. Bao, Nat. Mater **9**, 859 (2010).
53 S. Wan, H. Bi, Y. Zhou, X. Xie, S. Su, K. Yin, and L. Sun, Carbon **114**, 209 (2017).
54 Y. Liu, L. Q. Tao, D. Y. Wang, T. Y. Zhang, Y. Yang, and T. L. Ren, Appl. Phys. Lett. **110**, 123508 (2017).
55 S. E. Zhu, M. Krishna Ghatkesar, C. Zhang, and G. C. A. M. Janssen, Appl. Phys. Lett. **102**, 161904 (2013).
56 R. J. Grow, Q. Wang, J. Cao, D. Wang, and H. Dai, Appl. Phys. Lett. **86**, 093104 (2005).
57 B. Zhu, Z. Niu, H. Wang, W. R. Leow, H. Wang, Y. Li, L. Zheng, J. Wei, F. Huo, and X. Chen, Small **10**, 3625 (2014).
58 H. Tian, Y. Shu, X. F. Wang, M. A. Mohammad, Z. Bie, Q. Y. Xie, C. Li, W. T. Mi, Y. Yang, and T. L. Ren, Sci. Rep. **5**, 8603 (2015).
59 C. T. Lee, and Y. S. Chiu, Appl. Phys. Lett. **106**, 073502 (2015).
60 C. L. Choong, M. B. Shim, B. S. Lee, S. Jeon, D. S. Ko, T. H. Kang, J. Bae, S. H. Lee, K. E. Byun, J. Im, Y. J. Jeong, C. E. Park, J. J. Park, and U. I. Chung, Adv. Mater. **26**, 3451 (2014).
61 C. M. Boutry, A. Nguyen, Q. O. Lawal, A. Chortos, S. Rondeau-Gagné, and Z. Bao, Adv. Mater. **27**, 6954 (2015).
62 J. Kim, M. Lee, H. J. Shim, R. Ghaffari, H. R. Cho, D. Son, Y. H. Jung, M. Soh, C. Choi, S. Jung, K. Chu, D. Jeon, S. T. Lee, J. H. Kim, S. H. Choi, T. Hyeon, and D. H. Kim, Nat. Commun. **5**, 5747 (2014).
63 Y. Zang, F. Zhang, D. Huang, X. Gao, C. A. Di, and D. Zhu, Nat. Commun. **6**, 6269 (2015).
64 D. Kang, P. V. Pikhitsa, Y. W. Choi, C. Lee, S. S. Shin, L. Piao, B. Park, K. Y. Suh, T. I. Kim, and M. Choi, Nature **516**, 222 (2014).
65 S. Jung, J. Lee, T. Hyeon, M. Lee, and D. H. Kim, Adv. Mater. **26**, 6329 (2014).
66 C. Pang, J. H. Koo, A. Nguyen, J. M. Caves, M. G. Kim, A. Chortos, K. Kim, P. J. Wang, J. B. H. Tok, and Z. Bao, Adv. Mater. **27**, 634 (2015).
67 D. Carrera, B. Rossi, D. Zambon, P. Fragneto, and G. Boracchi, in *ECG Monitoring in Wearable Devices by Sparse Models*: Proceedings of European Conference on Machine Learning and Knowledge Discovery in Databases, Riva del Garda, Italy, 19-23 September, 2016, 9853, pp. 145-160, doi: 10.1007/978-3-319-46131-1_21.
68 J. Y. Baek, J. H. An, J. M. Choi, K. S. Park, and S. H. Lee, Sens.s Actuators A-Phys. **143**, 423 (2008).
69 P. S. Pandian, K. Mohanavelu, K. P. Safeer, T. M. Kotresh, D. T. Shakunthala, P. Gopal, and V. C. Padaki, Med. Eng. Phys. **30**, 466 (2008).
70 S. M. Lee, K. S. Sim, K. K. Kim, Y. G. Lim, and K. S. Park, Med. Biol. Eng. Comput. **48**, 447 (2010).
71 H. C. Jung, J. H. Moon, D. H. Baek, J. H. Lee, Y. Y. Choi, J. S. Hong, and S. H. Lee, IEEE Trans. Biomed. Eng. **59**, 1472 (2012).
72 X. F. Pu, L. Wan, H. Zhang, Y. J. Qin, and Z. L. Hong, J. Semicond. **34**, 055002 (2013).
73 Z. Liu, and X. Liu, J. Text. Sci. Tech. **01**, 110 (2015).
74 C. Lou, R. Li, Z. Li, T. Liang, Z. Wei, M. Run, X. Yan, and X. Liu, Sensors **16**, 1833 (2016).

75 J. S. Lee, J. Heo, W. K. Lee, Y. G. Lim, Y. H. Kim, and K. S. Park, Sensors **14**, 14732 (2014).
76 Y. Meng, Z. Li, and J. Chen, Microsyst. Technol. **22**, 2027 (2015).
77 B. Liu, Z. Luo, W. Zhang, Q. Tu, and X. Jin, Sens. Actuators A-Phys. **247**, 459 (2016).
78 M. K. Yapici, T. Alkhidir, Y. A. Samad, and K. Liao, Sens. Actuators B-Chem. **221**, 1469 (2015).
79 S. M. Lee, H. J. Byeon, J. H. Lee, D. H. Baek, K. H. Lee, J. S. Hong, and S. H. Lee, Sci. Rep. **4**, 6074 (2014).
80 S. Imani, A. J. Bandodkar, A. M. V. Mohan, R. Kumar, S. Yu, J. Wang, and P. P. Mercier, Nat. Commun. **7**, 11650 (2016).
81 F. Cai, C. Yi, S. Liu, Y. Wang, L. Liu, X. Liu, X. Xu, and L. Wang, Biosens. Bioelectron. **77**, 907 (2016).
82 Y. Khan, M. Garg, Q. Gui, M. Schadt, A. Gaikwad, D. Han, N. A. D. Yamamoto, P. Hart, R. Welte, W. Wilson, S. Czarnecki, M. Poliks, Z. Jin, K. Ghose, F. Egitto, J. Turner, and A. C. Arias, Adv. Funct. Mater. **26**, 8764 (2016).
83 R. Barea, L. Boquete, S. Ortega, E. López, and J. M. Rodríguez-Ascariz, Expert Syst. Appl. **39**, 2677 (2012).
84 H. L. Peng, H. L. Jing-Quan Liu, H. C. Tian, Y. Z. Dong, B. Yang, X. Chen, and C. S. Yang, Sens. Actuators B-Chem. **226**, 349 (2016).
85 D. H. Kim, N. Lu, R. Ma, Y. S. Kim, R. H. Kim, S. Wang, J. Wu, S. M. Won, H. Tao, A. Islam, K. J. Yu, T. Kim, R. Chowdhury, M. Ying, L. Xu, M. Li, H. J. Chung, H. Keum, M. McCormick, P. Liu, Y. W. Zhang, F. G. Omenetto, Y. Huang, T. Coleman, and J. A. Rogers, Science **333**, 838 (2011).
86 X. Guo, W. Pei, Y. Wang, Y. Chen, H. Zhang, X. Wu, X. Yang, H. Chen, Y. Liu, and R. Liu, BioMed. Signal Processing Control **30**, 98 (2016).
87 B. Xu, A. Akhtar, Y. Liu, H. Chen, W. H. Yeo, S. I. Park, B. Boyce, H. Kim, J. Yu, H. Y. Lai, S. Jung, Y. Zhou, J. Kim, S. Cho, Y. Huang, T. Bretl, and J. A. Rogers, Adv. Mater. **28**, 4462 (2016).
88 J. W. Jeong, W. H. Yeo, A. Akhtar, J. J. S. Norton, Y. J. Kwack, S. Li, S. Y. Jung, Y. Su, W. Lee, J. Xia, H. Cheng, Y. Huang, W. S. Choi, T. Bretl, and J. A. Rogers, Adv. Mater. **25**, 6839 (2013).
89 H. Stein, and K. Firestone, Seminars Fetal Neonatal Med. **19**, 60 (2014).
90 T. Allsop, T. Earthrowl-Gould, D. J. Webb, and I. Bennion, J. Biomed. Opt. **8**, 552 (2003).
91 D. E. Becker, and A. B. Casabianca, Anesthesia Prog. **56**, 14 (2009).
92 J. De jonckheere, F. Narbonneau, L.T. D'Angelo, J. Witt, B. Paquet, D. Kinet, K. Kreber, and R. Logier, in *FBG-based smart textiles for continuous monitoring of respiratory movements for healthcare applications*: Proceedings of 12th IEEE International Conference o ne-Health Networking Applications and Services (Healthcom), Lyon, France, 1-3 July 2010, pp. 277-282, doi:10.1109/HEALTH.2010.5556557.
93 W. Y. Chang, C. C. Huang, C. C. Chen, C. C. Chang, and C. L. Yang, Sensors **14**, 22021 (2014).
94 P. Jiang, S. Zhao, and R. Zhu, Sensors **15**, 31738 (2015).
95 Z. Liu, S. Zhang, Y. M. Jin, H. Ouyang, Y. Zou, X. X. Wang, L. X. Xie, and Z. Li, Semicond. Sci. Technol. **32**, 064004 (2017).
96 T. Ono, H. Takegawa, T. Ageishi, M. Takashina, H. Numasaki, M. Matsumoto, and T. Teshima, Phys. Med. Biol. **56**, 6279 (2011).
97 M. Krehel, M. Schmid, R. M. Rossi, L. F. Boesel, G. L. Bona, and L. J. Scherer, Sensors **14**, 13088 (2014).
98 S. T. A. Hamdani, and A. Fernando, Sensors **15**, 7742 (2015).
99 P. Janik, M. A. Janik, and Z. Wróbel, Sens. Actuators A-Phys. **239**, 79 (2016).
100 A. Nag, S. C. Mukhopadhyay, and J. Kosel, Sens. Actuators A-Phys. **251**, 148 (2016).
101 P. Xiao, L. I. Ciortea, H. Singh, E. P. Berg, and R. E. Imhof, J. Phys.-Conf. Ser. **214**, 012008 (2010).
102 R. C. Webb, R. M. Pielak, P. Bastien, J. Ayers, J. Niittynen, J. Kurniawan, M. Manco, A. Lin, N. H. Cho, V. Malyrchuk, G. Balooch, and J. A. Rogers, PLoS ONE **10**, e0118131 (2015).
103 H. Tagami, M. Ohi, K. Iwatsuki, Y. Kanamaru, M. Yamada, and B. Ichijo, J. Invest. Dermatology **75**, 500 (1980).
104 P. Clarys, A. O. Barel, and B. Gabard, Skin Res. Tech. **5**, 14 (1999).
105 S. I. Alekseev, O. V. Gordiienko, and M. C. Ziskin, Bioelectromagnetics **29**, 340 (2008).
106 T. Yamamoto, and Y. Yamamoto, Med. Biol. Engng. **14**, 151 (1976).
107 R. L. Gunter, W. D. Delinger, T. L. Porter, R. Stewart, and J. Reed, Med. Eng. Phys. **27**, 215 (2005).
108 R. Stewart, J. Reed, J. Zhong, K. Morton, and T. L. Porter, Med. Eng. Phys. **29**, 1084 (2007).
109 X. Huang, W. H. Yeo, Y. Liu, and J. A. Rogers, Biointerphases **7**, 52 (2012).
110 Y. Zhou, H. Han, H. P. P. Naw, A. V. Lammy, C. H. Goh, S. Boujday, and T. W. J. Steele, Mater. Des. **90**, 1181 (2016).
111 X. Huang, Y. Liu, H. Cheng, W. J. Shin, J. A. Fan, Z. Liu, C. J. Lu, G. W. Kong, K. Chen, D. Patnaik, S. H. Lee, S. Hage-Ali, Y. Huang, and J. A. Rogers, Adv. Funct. Mater. **24**, 3846 (2014).
112 S. Yao, A. Myers, A. Malhotra, F. Lin, A. Bozkurt, J. F. Muth, and Y. Zhu, Adv. Healthcare Mater. **6**, 1601159 (2017).
113 S. Krishnan, Y. Shi, R. C. Webb, Y. Ma, P. Bastien, K. E. Crawford, A. Wang, X. Feng, M. Manco, J. Kurniawan, E. Tir, Y. Huang, G. Balooch, R. M. Pielak, and J. A. Rogers, Microsyst. Nanoeng. **3**, 17014 (2017).
114 H. Cheng, Y. Zhang, X. Huang, J. A. Rogers, and Y. Huang, Sens. Actuators A-Phys. **203**, 149 (2013).
115 B. Schazmann, D. Morris, C. Slater, S. Beirne, C. Fay, R. Reuveny, N. Moyna, and D. Diamond, Anal. Methods **2**, 342 (2010).
116 M. Ngoepe, Y. E. Choonara, C. Tyagi, L. K. Tomar, L. C. du Toit, P. Kumar, V. M. K. Ndesendo, and V. Pillay, Sensors **13**, 7680 (2013).
117 A. J. Bandodkar, D. Molinnus, O. Mirza, T. Guinovart, J. R. Windmiller, G. Valdés-Ramírez, F. J. Andrade, M. J. Schöning, and J. Wang, Biosens. Bioelectron. **54**, 603 (2014).
118 J. T. J. Huang, F. M. Leweke, D. Oxley, L. Wang, N. Harris, D. Koethe, C. W. Gerth, B. M. Nolden, S. Gross, D. Schreiber, B. Reed, and S. Bahn, PLoS Med. **3**, e428 (2006).
119 D. T. Wong, J. Am. Dental Association **137**, 313 (2006).
120 B. S. Kwak, H. O. Kim, J. H. Kim, S. Lee, and H. I. Jung, Biosens. Bioelectron. **35**, 484 (2012).
121 M. Parrilla, R. Cánovas, I. Jeerapan, F. J. Andrade, and J. Wang, Adv. Healthcare Mater. **5**, 996 (2016).
122 A. Cazalé, W. Sant, F. Ginot, J. C. Launay, G. Savourey, F. Revol-Cavalier, J. M. Lagarde, D. Heinry, J. Launay, and P. Temple-Boyer, Sens. Actuators B-Chem. **225**, 1 (2016).
123 T. Guinovart, A. J. Bandodkar, J. R. Windmiller, F. J. Andrade, and J. Wang, Analyst **138**, 7031 (2013).
124 P. Labroo, and Y. Cui, Biosens. Bioelectron. **41**, 852 (2013).
125 E. L. Tur-García, F. Davis, S. D. Collyer, J. L. Holmes, H. Barr, and S. P. J. Higson, Sens. Actuators B-Chem. **242**, 502 (2017).
126 V. A. T. Dam, M. A. G. Zevenbergen, and R. van Schaijk, Procedia Eng. **120**, 237 (2015).
127 H. Kudo, T. Sawada, E. Kazawa, H. Yoshida, Y. Iwasaki, and K. Mitsubayashi, Biosens. Bioelectron. **22**, 558 (2006).
128 M. Schaefer, M. Schellenberg, U. Merle, K. H. Weiss, and W. Stremmel, BMC Gastroenterol **8**, 1 (2008).
129 P. J. Derbyshire, H. Barr, F. Davis, and S. P. J. Higson, J. Physiol. Sci. **62**, 429 (2012).
130 S. M. Shirreffs, and R. J. Maughan, J. Appl. Physiol. **82**, 336 (1997).
131 J. Choi, Y. Xue, W. Xia, T. R. Ray, J. T. Reeder, A. J. Bandodkar, D. Kang, S. Xu, Y. Huang, and J. A. Rogers, Lab Chip **17**, 2572 (2017).
132 J. Choi, D. Kang, S. Han, S. B. Kim, and J. A. Rogers, Adv. Healthcare Mater. **6**, 1601355 (2017).
133 M. Caldara, C. Colleoni, E. Guido, V. Re, and G. Rosace, Sens. Actuators B-Chem. **222**, 213 (2016).
134 S. Coyle, S. King-Tong Lau, N. Moyna, D. O'Gorman, D. Diamond, F. Di Francesco, D. Costanzo, P. Salvo, M. G. Trivella, D. E. De Rossi, N. Taccini, R. Paradiso, J. A. Porchet, A. Ridolfi, J. Luprano, C. Chuzel, T. Lanier, F. Revol-Cavalier, S. Schoumacker, V. Mourier, I. Chartier, R. Convert, H. De-Moncuit, and C. Bini, IEEE Trans.

Inform. Technol. Biomed. **14**, 364 (2010).
135 H. Lee, T. K. Choi, Y. B. Lee, H. R. Cho, R. Ghaffari, L. Wang, H. J. Choi, T. D. Chung, N. Lu, T. Hyeon, S. H. Choi, and D. H. Kim, Nat. Nanotech. **11**, 566 (2016).
136 W. Gao, S. Emaminejad, H. Y. Y. Nyein, S. Challa, K. Chen, A. Peck, H. M. Fahad, H. Ota, H. Shiraki, D. Kiriya, D. H. Lien, G. A. Brooks, R. W. Davis, and A. Javey, Nature **529**, 509 (2016).
137 W. Gao, H. Y. Y. Nyein, Z. Shahpar, H. M. Fahad, K. Chen, S. Emaminejad, Y. Gao, L. C. Tai, H. Ota, E. Wu, J. Bullock, Y. Zeng, D. H. Lien, and A. Javey, ACS Sens. **1**, 866 (2016).
138 X. Huang, Y. Liu, K. Chen, W. J. Shin, C. J. Lu, G. W. Kong, D. Patnaik, S. H. Lee, J. F. Cortes, and J. A. Rogers, Small **10**, 3083 (2014).
139 K. Chen, R. He, X. Luo, P. Qin, L. Tan, Y. Tang, and Z. Yang, Biosens. Bioelectron. **94**, 609 (2017).
140 D. M. Kim, S. J. Cho, C. H. Cho, K. B. Kim, M. Y. Kim, and Y. B. Shim, Biosens. Bioelectron. **79**, 165 (2016).
141 P. Salvo, N. Calisi, B. Melai, B. Cortigiani, M. Mannini, A. Caneschi, G. Lorenzetti, C. Paoletti, T. Lomonaco, A. Paolicchi, I. Scataglini, V. Dini, M. Romanelli, R. Fuoco, and F. Di Francesco, Biosens. Bioelectron. **91**, 870 (2017).
142 H. Lee, C. Song, Y. S. Hong, M. S. Kim, H. R. Cho, T. Kang, K. Shin, S. H. Choi, T. Hyeon, and D. H. Kim, Sci. Adv. **3**, e1601314 (2017).
143 S. Anastasova, B. Crewther, P. Bembnowicz, V. Curto, H. M. Ip, B. Rosa, and G. Z. Yang, Biosens. Bioelectron. **93**, 139 (2017).
144 X. Wang, Y. Gu, Z. Xiong, Z. Cui, and T. Zhang, Adv. Mater. **26**, 1336 (2014).
145 Y. Gao, H. Ota, E. W. Schaler, K. Chen, A. Zhao, W. Gao, H. M. Fahad, Y. Leng, A. Zheng, F. Xiong, C. Zhang, L. C. Tai, P. Zhao, R. S. Fearing, and A. Javey, Adv. Mater. **29**, 1701985 (2017).
146 J. Kim, P. Gutruf, A. M. Chiarelli, S. Y. Heo, K. Cho, Z. Xie, A. Banks, S. Han, K. I. Jang, J. W. Lee, K. T. Lee, X. Feng, Y. Huang, M. Fabiani, G. Gratton, U. Paik, and J. A. Rogers, Adv. Funct. Mater. **27**, 1604373 (2017).
147 J. K. Song, D. Son, J. Kim, Y. J. Yoo, G. J. Lee, L. Wang, M. K. Choi, J. Yang, M. Lee, K. Do, J. H. Koo, N. Lu, J. H. Kim, T. Hyeon, Y. M. Song, and D. H. Kim, Adv. Funct. Mater. **27**, 1605286 (2017).
148 R. Li, H. Cheng, Y. Su, S. W. Hwang, L. Yin, H. Tao, M. A. Brenckle, D. H. Kim, F. G. Omenetto, J. A. Rogers, and Y. Huang, Adv. Funct. Mater. **23**, 3106 (2013).
149 S. W. Hwang, S. K. Kang, X. Huang, M. A. Brenckle, F. G. Omenetto, and J. A. Rogers, Adv. Mater. **27**, 47 (2015).
150 S. K. Kang, S. W. Hwang, S. Yu, J. H. Seo, E. A. Corbin, J. Shin, D. S. Wie, R. Bashir, Z. Ma, and J. A. Rogers, Adv. Funct. Mater. **25**, 1789 (2015).
151 S. W. Hwang, H. Tao, D. H. Kim, H. Cheng, J. K. Song, E. Rill, M. A. Brenckle, B. Panilaitis, S. M. Won, Y. S. Kim, Y. M. Song, K. J. Yu, A. Ameen, R. Li, Y. Su, M. Yang, D. L. Kaplan, M. R. Zakin, M. J. Slepian, Y. Huang, F. G. Omenetto, and J. A. Rogers, Science **337**, 1640 (2012).
152 C. Dagdeviren, S. W. Hwang, Y. Su, S. Kim, H. Cheng, O. Gur, R. Haney, F. G. Omenetto, Y. Huang, and J. A. Rogers, Small **9**, 3398 (2013).
153 S. W. Hwang, D. H. Kim, H. Tao, T. Kim, S. Kim, K. J. Yu, B. Panilaitis, J. W. Jeong, J. K. Song, F. G. Omenetto, and J. A. Rogers, Adv. Funct. Mater. **23**, 4087 (2013).
154 S. W. Hwang, X. Huang, J. H. Seo, J. K. Song, S. Kim, S. Hage-Ali, H. J. Chung, H. Tao, F. G. Omenetto, Z. Ma, and J. A. Rogers, Adv. Mater. **25**, 3526 (2013).
155 C. H. Lee, S. K. Kang, G. A. Salvatore, Y. Ma, B. H. Kim, Y. Jiang, J. S. Kim, L. Yan, D. S. Wie, A. Banks, S. J. Oh, X. Feng, Y. Huang, G. Troester, and J. A. Rogers, Adv. Funct. Mater. **25**, 5100 (2015).
156 D. H. Kim, R. Ghaffari, N. Lu, S. Wang, S. P. Lee, H. Keum, R. D'Angelo, L. Klinker, Y. Su, C. Lu, Y. S. Kim, A. Ameen, Y. Li, Y. Zhang, B. de Graff, Y. Y. Hsu, Z. Liu, J. Ruskin, L. Xu, C. Lu, F. G. Omenetto, Y. Huang, M. Mansour, M. J. Slepian, and J. A. Rogers, Proc. Natl. Acad. Sci. USA **109**, 19910 (2012).
157 T. Lei, M. Guan, J. Liu, H. C. Lin, R. Pfattner, L. Shaw, A. F. McGuire, T. C. Huang, L. Shao, K. T. Cheng, J. B. H. Tok, and Z. Bao, Proc. Natl. Acad. Sci. USA **114**, 5107 (2017).